AD-A041 110 NEW MEXICO STATE UNIV UNIVERSITY PARK DEPT OF PHYSICS F/G 7/4
RELATIONS AMONG KUBELKA-MUNK COEFFICIENTS AND ABSORPTION AND SC--ETC(U)
APR 77 G H GOEDECKE, M RAHMAN DAAG29-76-G-0077
UNCLASSIFIED NMSU-PHYS-76-00003 ARO-13542.1-GSX NL

4 OF 4
AD
A041110

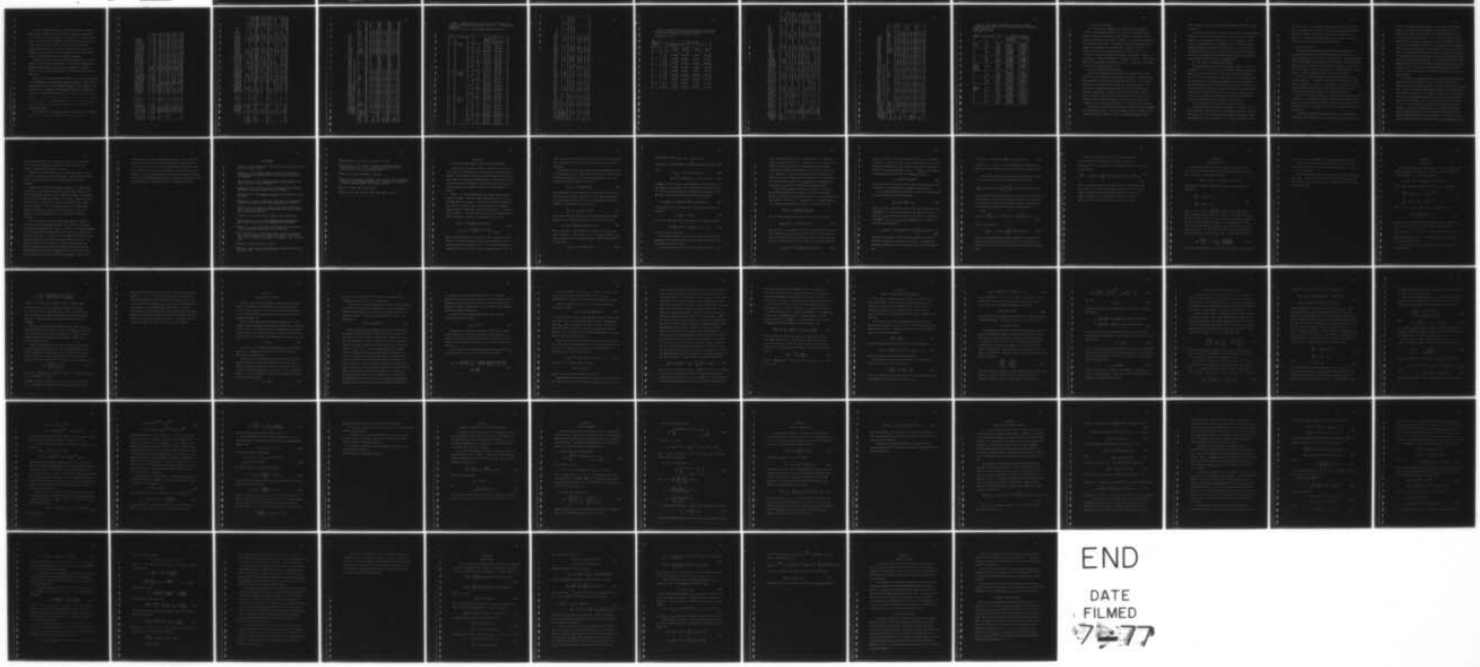

END

DATE
FILMED
7-77

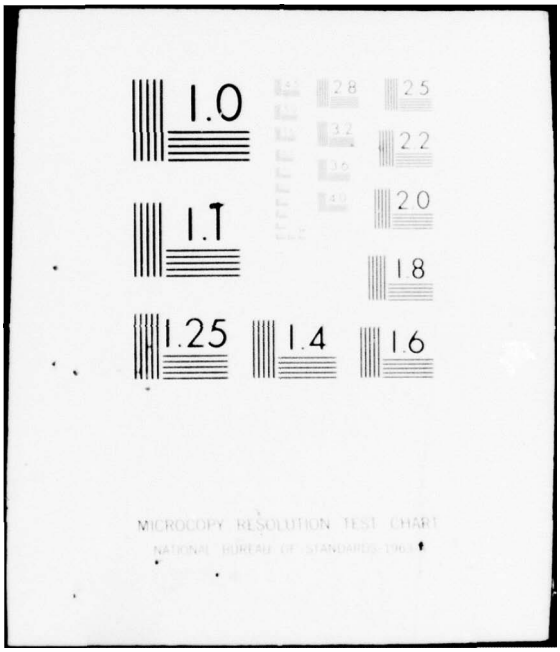
1.0
1.1
1.25
1.4
1.6
2.8
2.5
3.2
2.2
3.6
2.0
4.0
1.8
MICROCOPY RESOLUTION TEST CHART
NATIONAL BUREAU OF STANDARDS-1963-A

NMSU-PHYS-76-00003

ARO-13542.1-GSX

12

RELATIONS AMONG KUBELKA-MUNK COEFFICIENTS AND ABSORPTION AND SCATTERING COEFFICIENTS OF POWDERS

Final Report

CONTRACT DAAG-29-76-G-0077

Contract Period 1 January 1976 through 28 February 1977

Prepared for

United States Army Research Office

Post Office Box 12211

Research Triangle Park, NC 27709

76 Pages

UNCLASSIFIED

Approved for public release; distribution unlimited

Submitted by

G.H. Goedecke, Professor of Physics

M. Rahman, Postdoctoral Research Associate

PHYSICS DEPARTMENT
NEW MEXICO STATE UNIVERSITY
LAS CRUCES, NEW MEXICO 88003

402 005

SECURITY CLASSIFICATION OF THIS PAGE (When Data Entered)

(14) **REPORT DOCUMENTATION PAGE**

READ INSTRUCTIONS BEFORE COMPLETING FORM

1. REPORT NUMBER: NMSU-PHYS-76-00003
2. GOVT ACCESSION NO. (9)
3. RECIPIENT'S CATALOG NUMBER

4. TITLE (and Subtitle) (6): Relations among Kubelka-Munk Coefficients and Absorption and Scattering Coefficients of Powders,

5. TYPE OF REPORT & PERIOD COVERED: Final, technical rept. 1 Jan 76 - 28 Feb 77
6. PERFORMING ORG. REPORT NUMBER

7. AUTHOR(s) (10): G. H. Goedecke, M. Rahman

8. CONTRACT OR GRANT NUMBER(s) (15): DAAG29-76-G-0077 new

9. PERFORMING ORGANIZATION NAME AND ADDRESS: New Mexico State University, Las Cruces, NM 88003

10. PROGRAM ELEMENT, PROJECT, TASK AREA & WORK UNIT NUMBERS

11. CONTROLLING OFFICE NAME AND ADDRESS: U. S. Army Research Office, Post Office Box 12211, Research Triangle Park, NC 27709

(11) 20 April 1977

12. NUMBER OF PAGES: 76

14. MONITORING AGENCY NAME & ADDRESS (if different from Controlling Office)

(12) 75p.

15. SECURITY CLASS. (of this report): Unclassified

15a. DECLASSIFICATION/DOWNGRADING SCHEDULE: NA

16. DISTRIBUTION STATEMENT (of this Report)

(18) ARO

Approved for public release; distribution unlimited.

17. DISTRIBUTION STATEMENT (of the abstract entered in Block 20, if different from Report)

(19) 13542.1-GSX

NA

18. SUPPLEMENTARY NOTES

The findings in this report are not to be construed as an official Department of the Army position, unless so designated by other authorized documents.

19. KEY WORDS (Continue on reverse side if necessary and identify by block number)

Radiative Transfer Theory
Mie Theory
Kubelka-Munk Theory

20. ABSTRACT (Continue on reverse side if necessary and identify by block number)

The use of the Kubelka-Munk (KM) theory to predict absorption and scattering coefficients of powders from values of diffuse reflectance of an incident radiation beam is shown to lead to errors of 20% or less, for realistic model powders. The use of a conventional plausible relation to predict imaginary refractive index from absorption coefficient is found to produce errors of the order of 200%. Methods for correcting these errors are discussed. A new radiative transfer equation is derived and analyzed for applications to close-packed strongly absorbing or strongly reflecting media. For such media, the new equation predicts reflectances and transmittances which are

next page

DD FORM 1 JAN 73 1473 EDITION OF 1 NOV 65 IS OBSOLETE

Unclassified

SECURITY CLASSIFICATION OF THIS PAGE (When Data Entered)

402005

cont

Block 20. (continued)

significantly different from those predicted by the standard transfer equation.

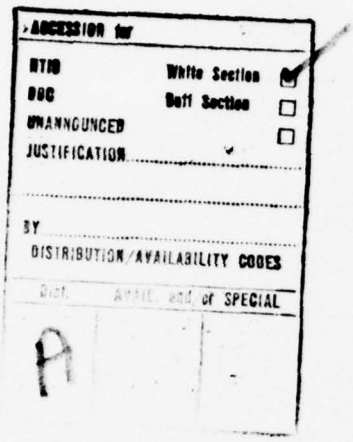

CONTENTS

	Page
Introduction	1
Summary of Results and Prognosis	2
Glossary of Symbols	4
Computer Modelling of Powders	5
Method	5
Results	7
Discussion of Results	18
Theoretical Studies	20
Bibliography	24
Appendixes	26

TABLES AND APPENDIXES

Page

Table 1. Model sample parameters 9

Table 2. Mie Theory parameters, wavelength 0.6 μm. 10

Table 3. Kubelka-Munk Theory results, 0.6 μm 11

Table 4. Diffuse reflectances, 0.6 μm 12

Table 5. Near field vs. far field Kubelka-Munk coefficients, 0.6 μm 13

Table 6. Near field vs. far field reflectances, 0.6 μm . . . 14

Table 7. Mie Theory parameters, wavelength 1.0 μm 15

Table 8. Kubelka-Munk theory results, 1.0 μm 16

Table 9. Diffuse reflectances, 1.0 μm 17

Appendix A. Radiative Transfer Theory and Near Field Phase Functions 26

Appendix B. Kubelka-Munk Theory 33

Appendix C. Reichman Theory. 35

Appendix D. Relation between κ and α 38

Appendix E. Radiative Transfer Theory in One Dimension . . . 44

Appendix F. Conversion of Fraction by Weight to Number Density 54

Appendix G. Size Distributions 55

Appendix H. $p^{(o)}(\mu,\mu')$ from $p(\cos\theta)$ 57

Appendix I. New Equation of Radiative Transfer 59

Appendix J. Doubling Method. 68

Appendix K. Computer Programs 72

I. Introduction

The major objective of the theoretical investigation reported here was to obtain relations between the actual absorption and scattering coefficients of powders, and the predictions of these coefficients which are often made by applying the Kubelka-Munk (KM) theory[1] to measured values of diffuse reflectance from powder samples. Another objective was to evaluate one of the conventional methods for obtaining imaginary refractive indices from absorption coefficients, and to suggest and implement corrections to this method, if possible. A third objective was to ascertain to what extent the standard Mie theory and radiative transfer theory predictions of diffuse reflectances from model powder samples agree with experimental results from corresponding actual powder samples.

The first and second objectives above were partially attained. The results of the investigation show that the KM theory predicts values of absorption and scattering coefficients that are sensitive to incident beam direction and sample optical depth, and that the abovementioned method for conversion from absorption coefficients to imaginary refractive indices is subject to large errors. However, the third objective mentioned above was not achieved, inasmuch as actual experimental results from powders which could be modelled easily were not available.

The investigation proceeded on two levels. The first level involved computer simulation of several realistic powder samples, using standard Mie theory and radiative transfer theory algorithms, which allowed numerical comparisons of predicted vs. actual absorption and scattering coefficients, and evaluation of the conventional relation between imaginary index and absorption coefficient. The second level involved the derivation and fundamental study of a new equation of radiative transfer, which should

be significantly more accurate than the standard one in practical application to closely packed random scattering media which contain strongly absorbing or strongly reflecting particles.

This report is structured for readers of three different levels of interest. The reader who needs only a synopsis just a bit more detailed than the abstract need consider only section II, with perhaps a reference to the glossary of symbols in section III. The reader who wants a look at the computational results, or at the theoretical concepts leading to the new equation of radiative transfer, can peruse sections IV and V. Finally, the reader who is interested in depth can delve into the appendixes.

Some of the material in this report will soon be submitted for publication in J. Opt. Soc. Am. and/or Applied Optics. It is planned to write two papers based on this investigation, one dealing with the new radiative transfer equations, the other with the computational results.

II. Summary of Results and Prognosis

A. Summary

The major results of this theoretical investigation are as follows:

1) The use of the Kubelka-Munk (KM) theory to obtain values of the absorption and back-scattering coefficients of random scattering media from diffuse reflectance data leads to errors $\lesssim$ 20%, over a range of incident beam angles. These errors result primarily because the KM theory neglects the effect of incident beam angle. The errors might be partially removed by making use of the Reichman theory.[2] See section IV and appendix C for details.

2) The use of the plausible hypothetical relation $\alpha = (Nv)(4\pi\kappa/\lambda)$, in order to determine a value of the imaginary index κ of a substance

from a presumed known value of the absorption coefficient α of a random scattering medium composed of particles of that substance, is subject to errors of a factor of two to three. In most cases, these large errors can be removed only by recourse to the full Mie theory relation between α and κ, which is very difficult to invert in general. See section IV and appendix D for details.

3) The use of the standard differential equation of radiative transfer for closely packed strongly reflecting or absorbing scattering media probably leads to significant error. For such media, the new difference equation of radiative transfer which was developed during this investigation should be used. The use of the in principle incorrect far field phase function, rather than a more nearly correct near field one, probably makes no pratical difference. See section V and appendixes E, A, I for details.

B. Prognosis

Future work in this area should include the following:

1) A thorough investigation of the new difference equation of radiative transfer, and comparison with the standard theory, for realistic close-packed model scattering media of practical interest. Such media include both highly reflecting and highly absorbing paints and coatings, powders containing strong reflectors or absorbers, and the like.

2) Another look at the conventional averaging over different kinds and sizes of particles in close-packed media composed of strongly absorbing or strongly reflecting particles. Preliminary consideration by the author indicates that the standard method of averaging (see appendix A) may lead to significant errors, for such media. In addition, the effects of polarized light and non-spherical scatterers should be evaluated.

3) An error analysis for the application of the Reichman theory (appendix C), rather than the KM theory, in reduction of experimental diffuse reflectance data, in cases where the incident beam angle is not near 60°.

4) An attempt to invert the Mie theory calculations, so that an imaginary and/or real index of refraction could be obtained easily and accurately from known values of the scattering and absorbtion cross-sections. (See appendix D).

III. Glossary of Symbols

$\lambda \equiv$ wavelength, μm

$(n_i, \kappa_i) \equiv$ (real, imaginary) refractive indices of i^{th} optical type in a random scattering medium

$m_i \equiv n_i - i\kappa_i$ = complex refractive index of ^{ith} particle type

$f_i(r) \equiv$ size distribution of spherical particles of type i as function of particle radius r; $\int dr\, f_i(r) = 1$

$N_i \equiv$ number density of particles of i^{th} type, μm^{-3}

$N \equiv$ total number density in medium = $\sum_i N_i$

$v_i \equiv \int dr\, f_i(r)(4\pi r^3/3) =$ average volume of i^{th} type particle, μm^3

$\sigma(\theta) \equiv$ differential scattering cross-section of the average particle in a medium as function of scattering angle θ

$\sigma(\underset{\sim}{s}, \underset{\sim}{s}') \equiv$ differential cross-section for scattering from direction $\underset{\sim}{s}'$ to direction $\underset{\sim}{s}$.

$(\sigma_{abs}, \sigma_{sca}, \sigma_{ext}) \equiv$ (absorption, scattering, extinction) cross-sections of an average particle in the medium, $(\mu m)^2$

$(\alpha, \beta, \gamma) \equiv$ (absorption, scattering, extinction) coefficient of the medium, μm^{-1}. $\alpha \equiv N\sigma_{abs}$, $\beta \equiv N\sigma_{sca}$, $\gamma \equiv N\sigma_{ext}$.

$\omega_o \equiv \beta/\gamma$ = single-scattering albedo of the medium.

$p(\theta) \equiv$ phase function of the medium. $p(\theta) \equiv 4\pi\sigma(\theta)/\sigma_{ext}$

$p^{(o)}(\mu,\mu') \equiv$ azimuth averaged phase function of the medium, as function of $\mu = \cos\theta$, $\mu' = \cos\theta'$, for scattering from direction θ' to direction θ. Here, θ, θ' are measured from the forward-direction normal to the plane surface of a sample.

$\beta_{\pm} \equiv \frac{1}{2}\gamma \int_o^1 d\mu \int_o^1 d\mu' \, p^{(o)}(\mu,\pm\mu') =$ average $\binom{\text{forward}}{\text{back}}$-scattering coefficient, μm^{-1}.

$D \equiv$ mass density of model powder, gm/cm^3.

$\rho_i \equiv$ mass density of type i powder constituent, gm/cm^3

$\theta_o \equiv$ angle of incident beam w.r. to the forward-direction plane surface normal to the sample.

$(K,S) \equiv$ Kubelka-Munk (KM) (absorption, scattering) coefficients, μm^{-1}. $K \equiv 2\alpha$, $S \equiv 2\beta-$.

$d \equiv$ Thickness of sample; optical thickness $\tau = \gamma d$.

$(\bar{K},\bar{S}) \equiv$ KM (absorption, scattering) coefficient evaluated from diffuse reflectance data, for each (θ_o,d) considered.

$R_d \equiv$ diffuse reflectance of a plane parallel sample of thickness d, on a black background.

$R_\infty \equiv$ diffuse reflectance of an infinitely thick sample.

IV. Computer Modelling of Powders

A. Method

Given the number densities, optical constants, and size distributions of the spherical particles in a random scattering medium, standard Mie theory algorithms[3] yield the quantities σ_{abs}, σ_{sca}, σ_{ext}, $\alpha,\beta,\gamma,\sigma(\theta)$ and $p(\theta)$. However, for closely packed media, such as powders, a given particle

sees the near zone or induction zone fields, rather than the radiation zone fields, from its neighbors. Therefore, it is likely that a suitably defined near field phase function should be used; see appendix A for details. In this work calculations were done with both the standard asymptotic phase function, and a near field phase function, and compared.

For an actual powder sample, the particle number densities N_i are not known *a priori*, but the total mass density and the fraction by weight of each constituent can be regarded as given. Appendix F details the conversion of these data to N_i.

In an actual powder, the size distributions of the various components are difficult to determine accurately. Only good estimates of the mean particle radius and the width of each distribution may be available. In modelling powders, therefore, recourse is made to several size distributions which are thought to be realistic. The various distributions used in this work are detailed in appendix G; these distributions have been used recently by other authors.[4] It is important to remark here that, for the computer modelling comparisons which are made in this work, the actual size distributions are irrelevant, since no comparisons are made with actual experimental data. However, realistic choices were made for the distribution parameters in the modelling.

From the phase function $p(\Theta)$, the azimuth averaged phase function $p^{(o)}(\mu,\mu')$ is found by the method detailed in appendix H. Since only total forward and backward radiation fluxes are needed in this work, only $p^{(o)}(\mu,\mu')$ is needed, rather than the full azimuth-dependent phase function.

Given $p^{(o)}(\mu,\mu')$, the thickness d of a plane parallel sample, and the incident radiation beam direction θ_o, standard radiative transfer theory

algorithms[5] yield the total diffuse reflectance and transmittance of the sample. The doubling method algorithms which were used in this work are detailed in appendix J; the relevant radiative transfer equation to which these were applied is given in appendix A, Eq. (A19). A method used by experimentalists[6,7] to obtain values of the absorption and scattering coefficients of a medium from diffuse reflectance data involves the Kubelka-Munk (KM) theory.[1] This theory is detailed in appendix B. In this investigation, the diffuse reflectances (R_d, R_∞), which were calculated as described above, were inserted into the KM relations (B2). The resulting quantities $\bar{K}(\theta_o, d)$, $\bar{S}(\theta_o, d)$ were compared with the known (calculated) values of $K \equiv 2\alpha$, $S \equiv 2\beta$, for each model powder considered.

A two-flux radiative transfer theory which takes incident beam direction into account has been developed by Reichman.[2] This theory is described in appendix C. In this invetigation, the accuracy of this theory was checked by comparing its predictions of R_d with those of the accurate doubling method. As discussed in appendix C, it appears that experimentalists might achieve better approximations to (K,S) by using measured values of (R_d, R_∞) with this Reichman theory than they can with the standard KM theory, if they are limited to an incident beam direction θ_o quite different from 60°.

The computer programs which were developed for this work are described briefly in appendix K. Complete documentation and listing is available from the author on request.

B. Results

Numerical results are reported here for a selected number of samples and wavelengths.

The three samples reported were constituted as follows: Sample 1, $BaSO_4$; Sample 2, $BaSO_4$ plus carbon; Sample 3, model dust + $BaSO_4$; that is, the model dust contained carbon, ammonium sulfate, and clay minerals. Table 1 gives the relevant parameter values which were assigned. These values were quoted[8] as typical for these material constituents of atmospheric dust aerosols. The $BaSO_4$ was included in all these model samples so that they would be realistic models of actual powder samples used in some diffuse reflectance spectroscopy experiments.

The $BaSO_4$ particles have a fairly narrow size distribution centered around 0.5 μm mean radius, approximately. The carbon and $(NH_4)_2SO_4$ are similarly sharply peaked, but are centered roughly around 0.25 μm radius. The clay minerals distribution is fairly broad, between 0.03 μm and 5.0 μm.

The values used for the refractive indices n, κ, and the mass densities ρ, are in agreement with those given in several handbooks, such as that of the Geological Society of America (GSA).[9] However, the GSA handbook lists the mass density of graphite as 2.267 gm/cm^3, significantly larger than the figure 1.7 gm/cm^3 which was used for carbon soot in this work. It was decided to use the lower value, the one quoted to this author as appropriate for soot. Again, it is worth emphasizing that the trends revealed by the following results are insensitive to the accuracy of the modelling of an actual powder sample.

The following tables display the results of the computer calculations for these model samples, at wavelengths λ = 0.6 μm and 1.0 μm.

Table 1. Optical constants (n,κ), percent by weight (p), mass density (ρ), and size distribution parameters for constituents of model samples. Mass density of each sample = 2 gm/cm^3. The optical constants at wavelengths 0.6 μm and 1.0 μm are almost identical, and were set equal in this work. The size distribution parameters (A,B,) are the (a,b) for the gamma distribution: (A,B,C) ≡ (a,r_{min},r_{max}) for the power law distribution; see appendix H.

Sample	Components	n	κ	p(%)	ρ (gm/cm^3)	Size Dist.	A	B	C	R1	R2
1	$BaSO_4$	1.64	10^{-8}	100	4.5	gamma	0.5	0.1	0.0	0.0	3.0
2	$BaSO_4$	1.64	10^{-8}	99.99	4.5	gamma	0.5	0.1	0.0	0.0	3.0
	Carbon	1.8	0.6	0.01	1.7	gamma	0.25	0.1	0.0	0.0	3.0
3	$BaSO_4$	1.64	10^{-8}	99.9	4.5	gamma	0.5	0.1	0.0	0.0	3.0
	Carbon	1.8	0.6	.0001	1.7	gamma	0.25	0.1	0.0	0.0	3.0
	$(NH_4)_2SO_4$	1.523	0.0	.04	1.77	gamma	0.25	0.1	0.0	0.0	3.0
	Clay	1.525	.001	.059	2.6	power	4.0	.03	5.0	.03	5.0

Table 2. Optical constants (n,κ), average volume of particles (v), number density (N), absorption, scattering, and extinction coefficients (α,β,γ), for constituents of model samples, and for each sample as a whole. The coefficient $\alpha' \equiv 4\pi$ Nv κ/λ is to be compared with α. Wavelength λ = 0.6 μm; mass density of each sample D = 2.0 gm/cm^3.

Sample	Components	n	κ	v $(\mu m)^3$	N $(\mu m)^{-3}$	α $(\mu m)^{-1}$	β $(\mu m)^{-1}$	γ $(\mu m)^{-1}$	α' $(\mu m)^{-1}$
1	$BaSO_4$	1.64	10^{-9}	10.18	4.366×10^{-2}	1.906×10^{-8}	0.51813	0.51813	9.309×10^{-9}
2	$BaSO_4$	1.64	10^{-9}	10.18	4.366×10^{-2}	1.906×10^{-8}	0.51807	0.51807	9.309×10^{-9}
	Carbon	1.8	0.6	3.142×10^{-2}	3.744×10^{-3}	5.2053×10^{-4}	4.2668×10^{-4}	9.4721×10^{-4}	1.4783×10^{-3}
	Mixture				4.74×10^{-2}	5.2055×10^{-4}	0.51850	0.51902	1.4783×10^{-3}
3	$BaSO_4$	1.64	10^{-9}	10.18	4.362×10^{-2}	1.9042×10^{-8}	0.51760	0.51760	9.300×10^{-9}
	Carbon	1.8	0.6	3.142×10^{-2}	3.744×10^{-4}	5.2053×10^{-5}	4.2668×10^{-5}	9.4721×10^{-5}	1.4783×10^{-4}
	$(NH_4)_2SO_4$	1.523	0.0	3.142×10^{-2}	1.439×10^{-2}	0.0	3.398×10^{-3}	3.398×10^{-3}	0.0
	Clay	1.525	10^{-3}	4.916×10^{-2}	9.232×10^{-3}	1.6917×10^{-5}	1.6153×10^{-3}	1.63224×10^{-3}	9.5053×10^{-6}
	Mixture				6.77×10^{-2}	6.897×10^{-5}	0.52266	0.52273	1.5735×10^{-4}

Table 3. The Kubelka-Munk coefficients $\overline{K}$, $\overline{S}$, evaluated from the KM relations (B2), for several angles of beam incidence and several optical depths of sample. $\overline{K}$ is to be compared with 2α, and $\overline{S}$ with $2\beta_-$.
Wavelength $\lambda = 0.6$ μm. Far field phase functions were used.

Sample	Optical Depth $\tau = \gamma d$	$\overline{K}(0°)_{-1}$ (μm)	$\overline{K}(12°)$	$\overline{K}(60°)$	2α	$\overline{S}(0°)_{-1}$ (μm)	$\overline{S}(12°)$	$\overline{S}(60°)$	β_-
1	16	3.5793×10^{-6}	3.5770×10^{-6}	2.7415×10^{-6}	3.8123×10^{-8}	0.08785	0.08797	0.14314	0.1016
$BaSO_4$	64	3.7264×10^{-6}	3.7231×10^{-6}	2.6285×10^{-6}		0.09167	0.09156	0.13723	
	256	3.7637×10^{-6}	3.7601×10^{-6}	2.6000×10^{-6}		0.09238	0.09247	0.13575	
2	16	1.2310×10^{-3}	1.2300×10^{-3}	0.9551×10^{-3}	1.0412×10^{-3}	0.08789	0.08801	0.14300	0.10171
$BaSO_4$	64	1.2843×10^{-3}	1.2829×10^{-3}	0.9150×10^{-3}		0.09169	0.09180	0.13700	
Carbon	256	1.2983×10^{-3}	1.2969×10^{-3}	0.9048×10^{-3}		0.09270	0.09280	0.13548	
3	16	1.6751×10^{-4}	1.6739×10^{-4}	1.2883×10^{-4}	1.3800×10^{-4}	0.08869	0.08882	0.14445	0.10267
$BaSO_4$	64	1.7451×10^{-4}	1.7433×10^{-4}	1.2349×10^{-4}		0.09240	0.09251	0.13847	
Dust	256	1.7638×10^{-6}	1.7619×10^{-4}	1.2214×10^{-4}		0.09339	0.09349	0.13695	

Table 4. Total diffuse reflectances for the model samples from the accurate multiple scattering calculations vs. the Reichman theory (appendix C).
Wavelength λ = 0.6 μm. Far field phase functions were used.

Sample	Components	τ	θ	Reflectances R_d	
				Multiple Scattering	Reichman
1	$BaSO_4$	16	0°	0.7306	0.8217
			12°	0.7309	0.8234
			60°	0.8155	0.8595
		64	0°	0.9184	0.9503
			12°	0.9185	0.9507
			60°	0.9441	0.9608
		256	0°	0.9773	0.9871
			12°	0.9774	0.9873
			60°	0.9845	0.9899
2	$BaSO_4$ Carbon	16	0°	0.7101	0.7976
			12°	0.7104	0.7995
			60°	0.7982	0.8397
		64	0°	0.8406	0.8745
			12°	0.8407	0.8756
			60°	0.8872	0.9003
		256	0°	0.8460	0.8758
			12°	0.8462	0.8769
			60°	0.8909	0.9013
3	$BaSO_4$ Dust	16	0°	0.7280	0.8186
			12°	0.7283	0.8203
			60°	0.8132	0.8570
		64	0°	0.9057	0.9370
			12°	0.9058	0.9375
			60°	0.9349	0.9502
		256	0°	0.9400	0.9533
			12°	0.9401	0.9537
			60°	0.9584	0.9631

Table 5. Near field vs. far field comparisons of $\overline{K}$, $\overline{S}$, for sample 2 ($BaSO_4$ plus carbon). Here, $\beta_{\pm} = \frac{1}{2}\gamma \int_0^1 d\mu \int_0^1 d\mu' p^{(o)}(\mu, \pm\mu')$, $\alpha = 5.2066 \times 10^{-4}$ μm^{-1}, $\beta = 0.51850$ μm^{-1}, $\gamma = 0.51902$ μm^{-1}. Wavelength $\lambda = 0.6$ μm.

τ	phase funct.	$\overline{K}(0°)$	$\overline{K}(12°)$	$\overline{K}(60°)$	$\overline{S}(0°)$	$\overline{S}(12°)$	$\overline{S}(60°)$	β_-	β_+
16	Far	1.2310×10^{-3}	1.2300×10^{-3}	0.9551×10^{-3}	0.08789	0.08801	0.14300	0.10171	0.41680
	Near	1.2309×10^{-3}	1.2229×10^{-3}	0.9637×10^{-3}	0.074462	0.075823	0.125856	0.09910	0.41939
64	Far	1.2843×10^{-3}	1.2829×10^{-3}	0.9150×10^{-3}	0.09169	0.09180	0.13700		
	Near	1.2979×10^{-3}	1.2840×10^{-3}	0.9184×10^{-3}	0.07852	0.07961	0.11946		
256	Far	1.2983×10^{-3}	1.2969×10^{-3}	0.9048×10^{-3}	0.09270	0.09280	0.13548		
	Near	1.3155×10^{-3}	1.3000×10^{-3}	0.9069×10^{-3}	0.07958	0.08060	0.11797		

Table 6. Near field vs. far field comparisons of reflectances given by the accurate multiple scattering calculation and by the Reichman theory for sample 2 ($BaSO_4$ plus Carbon).

Wavelength λ = 0.6 μm.

Optical depth $\gamma d \equiv \tau$	θ_o	Reflectances R_d			
		Multiple Scattering Theory		Reichman Theory	
		FAR	NEAR	FAR	NEAR
16	0°	0.7101	0.6769	0.7976	0.7938
	12°	0.7104	0.6807	0.7995	0.7951
	60°	0.7982	0.7776	0.8397	0.8321
64	0°	0.8406	0.8264	0.8745	0.8729
	12°	0.8407	0.8283	0.8756	0.8737
	60°	0.8872	0.8784	0.9003	0.8962
256	0°	0.8460	0.8340	0.8758	0.8744
	12°	0.8462	0.8358	0.8769	0.8752
	60°	0.8909	0.8835	0.9013	0.8974

Table 7. Optical constants (n,κ), average volume of particles (v), number density (N), absorption, scattering, and extinction coefficients (α, β,γ), for constituents of model samples, and for each sample as a whole. The coefficient $\alpha' \equiv 4\pi N v \kappa/\lambda$ is to be compared with α.
Wavelength $\lambda = 1.0$ μm. Mass density of each sample = 2.0 gm/cm^3.

Sample		n	κ	v $(\mu m)^3$	N $(\mu m)^{-3}$	α $(\mu m)^{-1}$	β $(\mu m)^{-1}$	γ $(\mu m)^{-1}$	α' $(\mu m)^{-1}$
1	$BaSO_4$	1.64	10^{-9}	10.18	4.366×10^{-2}	1.194×10^{-8}	0.54442	0.54442	5.585×10^{-9}
2	$BaSO_4$	1.64	10^{-9}	10.18	4.366×10^{-2}	1.194×10^{-8}	0.54437	0.54437	5.585×10^{-9}
	Carbon	1.8	0.6	3.142×10^{-2}	3.744×10^{-3}	4.8854×10^{-4}	3.357×10^{-4}	8.242×10^{-4}	8.87×10^{-4}
	Mixture				4.74×10^{-2}	4.8856×10^{-4}	0.54470	0.54519	8.87×10^{-4}
3	$BaSO_4$	1.64	10^{-9}	10.18	4.362×10^{-2}	1.193×10^{-8}	0.54387	0.54387	5.580×10^{-9}
	Carbon	1.8	0.6	3.142×10^{-2}	3.744×10^{-4}	4.885×10^{-5}	3.357×10^{-5}	8.242×10^{-5}	8.87×10^{-5}
	$(NH_4)_2SO_4$	1.523	0.0	3.142×10^{-2}	1.439×10^{-2}	0.0	1.5816×10^{-3}	1.5816×10^{-3}	0.0
	Clay	1.525	10^{-3}	4.916×10^{-2}	9.232×10^{-3}	9.827×10^{-6}	9.953×10^{-4}	1.005×10^{-3}	5.703×10^{-6}
	Mixture				6.76×10^{-2}	5.8704×10^{-5}	0.54649	0.54654	9.441×10^{-5}

Table 8. The Kubelka-Munk coefficients $\bar{K}, \bar{S}$, evaluated from the KM relations (B2), for several angles of beam incidence and several optical depths of sample. $\bar{K}$ is to be compared with 2α, S with $2\beta_-$.
Wavelength $\lambda = 1.0$ μm. Far field phase functions were used.

Sample	Optical Depth $\tau=\gamma d$	$\bar{K}(0°)_1$ (μm)	$\bar{K}(12°)$	$\bar{K}(60°)$	2α	$\bar{S}(0°)_1$ $(\mu m)^{-1}$	$\bar{S}(12°)$	$\bar{S}(60°)$	β_-
1	16	3.8028×10^{-6}	3.7675×10^{-6}	2.8483×10^{-6}	2.38798×10^{-8}	0.1060	0.1079	0.1727	0.1209
$BaSO_4$	64	3.9502×10^{-6}	3.9005×10^{-6}	2.7478×10^{-6}	2.38798×10^{-8}	0.1101	0.1118	0.1666	
	256	3.9876×10^{-6}	3.9343×10^{-6}	2.7225×10^{-6}	2.38798×10^{-8}	0.1111	0.1127	0.1650	
2	16	1.1746×10^{-3}	1.1643×10^{-3}	0.8918×10^{-3}	0.9773×10^{-3}	0.1061	0.1081	0.1726	0.1211
$BaSO_4$	64	1.2229×10^{-3}	1.2080×10^{-3}	0.8596×10^{-3}	0.9773×10^{-3}	0.1105	0.1122	0.1663	
Carbon	256	1.2356×10^{-3}	1.2196×10^{-3}	0.8514×10^{-3}	0.9773×10^{-3}	0.1116	0.1132	0.1647	
3	16	1.4557×10^{-4}	1.4424×10^{-4}	1.0949×10^{-4}	1.1741×10^{-4}	0.1065	0.1084	0.1734	0.1215
Dust	64	1.5130×10^{-4}	1.4942×10^{-4}	1.0560×10^{-4}	1.1741×10^{-4}	0.1107	0.1123	0.1672	
	256	1.5285×10^{-4}	1.5082×10^{-4}	1.0461×10^{-4}	1.1741×10^{-4}	0.1118	0.1134	0.1657	

Table 9. Total diffuse reflectances for the model samples, from the accurate multiple scattering calculations vs. the Reichman Theory (appendix C).
Wavelength λ = 1.0 μm.

Sample	Optical depth $\tau \equiv \gamma d$	θ_o	Reflectances R_d Multiple Scattering	Reichman
1 $BaSO_4$	16	0°	0.7570	0.8368
		12°	0.7603	0.8384
		60°	0.8354	0.8734
	64	0°	0.9280	0.9550
		12°	0.9290	0.9555
		60°	0.9512	0.9651
	256	0°	0.9800	0.9884
		12°	0.9803	0.9885
		60°	0.9864	0.9910
2 $BaSO_4$ and Carbon	16	0°	0.7381	0.8145
		12°	0.7415	0.8163
		60°	0.8198	0.8555
	64	0°	0.8572	0.8855
		12°	0.8590	0.8866
		60°	0.9002	0.9106
	256	0°	0.8619	0.8868
		12°	0.8636	0.8878
		60°	0.9034	0.9115
3 $BaSO_4$ Dust	16	0°	0.7548	0.8341
		12°	0.7581	0.8357
		60°	0.8335	0.8713
	64	0°	0.9174	0.9438
		12°	0.9185	0.9444
		60°	0.9437	0.9563
	256	0°	0.9487	0.9595
		12°	0.9493	0.9599
		60°	0.9648	0.9685

C. Discussion of Results

1) Relation between imaginary index and absorption coefficient. The discussion in appendix D shows that, in general, the plausible hypothetical relation $\alpha \stackrel{?}{=} Nv(4\pi\kappa/\lambda)$ is badly violated. The results in Tables 2 and 7 reinforce this conclusion; the values of α' vs. α show discrepancies of a factor of two or three. For example, following the reasoning in the latter part of appendix D, one could attempt to predict a value for κ of carbon, from the correct calculated value of α given in table 2, for $\lambda = 0.6$ μm., using the plausible relation above. From table 2, sample 2, for carbon, $v = 3.142 \times 10^{-2}$ $(\mu m)^3$, $N = 3.744 \times 10^{-3}$ $(\mu m)^{-3}$, $\alpha = 5.205 \times 10^{-4}$ $(\mu m)^{-1}$. The hypothetical relation above yields $\kappa = \lambda\ \alpha/4\pi\ Nv = 0.21$, rather than the correct (input) value $\kappa = 0.6$.

2) Relation between $(\bar{K},\bar{S})$ and (K,S).

Tables 3 and 8 display the values of $\bar{K},\bar{S}$ calculated from Eqs. (B2), using the accurate multiple scattering values of (R_d,R_∞). Experimentalists often hypothesize that these values should be equal to $(K \equiv 2\alpha,\ S \equiv 2\beta_-)$,[8] regardless of the beam angle of incidence or of the optical depth of the sample. The calculated results in these tables show that $(\bar{K},\bar{S})$ depend somewhat on both θ_o and d. However, in the cases of interest, samples 2 and 3, setting 2α equal to any of the $\bar{K}$ values leads to an error of less than 20%, which is probably acceptable at present. But the values of $\bar{S}$ seem much closer to β_- itself rather than to $2\beta_-$, the expected correlation.

The only large discrepancy between $\bar{K}$ and 2α occurred at both wavelengths for the pure $BaSO_4$ sample. Practically speaking, this is irrelevant, since the absorption due to $BaSO_4$ in a mixture is probably negligible in most

actual experimental cases, and is certainly negligible in the model samples treated here.

The computer calculations are accurate enough so that the above-mentioned discrepancies ($S \cong \beta_-$ rather than $2\beta_-$, $K >> 2\alpha$ for the very weak absorber $BaSO_4$) are probably real, not just artifacts of the arithmetic. If so, it may be conjectured that, since the model samples all contain closely packed $BaSO_4$ particles, which are strong reflectors, the origin of these discrepancies may just be what is discussed in appendixes E and I, namely, the failure in principle of the standard radiative transfer equations for closely packed strongly reflecting or absorbing media.

3) Near field vs. far field phase functions.

The underlying theory for the near field phase function is discussed in appendix A. Tables 5 and 6 present comparisons. Although the angular dependence of the near field phase functions is significantly different from that of the corresponding far field ones, the total reflectances were not very different, for the samples considered. Table 2 shows that the packing fraction, the ratio of the actual volume of an average particle to the average volume subtended per particle in the mixture, equal to Nv, was of the order 0.5 for these samples. It is possible that larger packing fractions would produce greater differences between near and far field predictions of reflectances; this remains for future work.

4) Reichman theory vs. full multiple scattering theory.

The Reichman theory[2] is discussed in appendix C. Tables 4, 6, and 9 give comparisons. The discrepancies are generally around 10%, so this two-flux theory, which takes into account the incident beam direction, could in principle be used to evaluate ($K \equiv 2\alpha$, $S \equiv 2\beta_-$) from reflectance data.

The formulas are more complicated than those of the KM theory, and more data is needed for each attempted evaluation, but more information about Mie theory parameters is obtained. Lacking an error analysis, it is difficult to estimate whether the Reichman theory would be more accurate in practical predictions of (K,S) than the KM theory.

IV. Theoretical Studies

The fundamental theoretical studies which were done during this investigation centered on the problem of multiple scattering in closely packed strongly absorbing or strongly reflecting media. Two major questions arise in this problem. The first question asks whether the standard differential equation of radiative transfer should be applicable to such media. The second, which arises only if the first is answered negatively, concerns whether a suitable equation of transfer can be found and solved.

In this work, the first question was answered negatively, and the second affirmatively. The detailed derivations and calculations are presented in appendixes E, A, and I. In appendix I, it is shown that the new radiative transfer equation should yield significantly different results than the standard equation, in many cases of practical interest.

Since the proposed new equation of radiative transfer may have practical consequences, it is important to achieve a thorough understanding of the logical steps which lead to the equation. For the interested reader, the logic pathway starts with appendix E, then goes to appendix A, then finally to appendix I.

In appendix E, a model one-dimensional random scattering medium is constructed. The medium consists of a stretched frictionless string, with

randomly but homogenously placed insertions of segments of a frictional string. This medium contains analogies to every major feature of a 3-dimensional random scattering medium. The wave motions are of course the transverse oscillations of the string. The exact equations for the intensity transfer through the medium, which are the complete analogs of the equations of radiative transfer in a 3-dimensional medium, are derived and solved without approximation. The equations turn out to be difference rather than differential equations; they reduce to differential equations of standard (two-flux theory) form only if the inserted scattering segments are very weak absorbers and reflectors. The exact solution of the correct difference equations for either strongly absorbing or strongly reflecting segments is quite different from the incorrect differential equation solution, and the expressions for transmittance and reflectance are also quite different.

In appendix A, the derivation of the usual 3-dimensional differential equation of radiative transfer[5] is done in an unusual manner which is partly analogous to the derivation done in appendix E for the one-dimensional case. Indeed, a difference equation (Eq. A6) arises in this derivation for the 3-dimensional case, and it is necessary to require $\gamma\ell << 1$ in order to achieve the usual differential equation (A9). Here, γ is the extinction coefficient of the medium, and ℓ is the average interparticle separation. If $\gamma\ell << 1$, then the change in intensity across a monoparticle layer is negligible. But if $\gamma\ell$ is not very small, there will be enough change across a monoparticle layer that the difference equation results will disagree with the differential equation results. The value of $\gamma\ell$ which should be used as a break point between the two equations depends of course

on the accuracy desired in a calculation. If accuracy ≃ 1% is desired, then the difference equation, rather than the standard differential equation, should probably be used if $\gamma\ell \gtrsim 0.01$.

Although a near field rather than a far field phase function should be used, in principle, for closely packed media, the computational results quoted in section IV imply that, practically speaking, the two are equivalent.

In appendix I, the difference equation analogs of Eqs. (A18), (A20) are derived. These difference equations are applicable to problems with (x-y) translational invariance in which azimuthal dependence is irrelevant, such as the problems which were treated in this work. Methods of solution are discussed; a combination of the many-flux method[10] and the doubling method is suggested. It is also conjectured that present Monte Carlo methods might already be solving the difference equation, since these methods treat the radiative transfer in discrete steps, collision by collision.

Also in appendix I, the two-flux difference equations, analogous to the KM equations, are developed and solved. The results are contrasted with the corresponding KM theory results. By means of two realistic examples, it is shown that the discrepancies between the two theories probably have practical significance. In fact, one of the examples involves the realistic $BaSO_4$ powder model which was used in the computations in this work. The parameter values in table 3 lead to $\beta\_\ell = 0.283$, indicating that the difference equations, rather than the differential equations, probably should have been used in all the computations which were reported! Time did not permit this; it is left for future investigation. However, the

principal source of error, in obtaining values of ($K \equiv 2\alpha$, $S \equiv 2\beta$) from diffuse reflectance data by means of the KM theory relations (B2), lies in the neglect of the incident beam angle dependence; this neglect would not be removed merely by use of the difference equation analog to the KM equations. And, of course, multiple scattering has nothing to do with the large error in the hypothetical relation $\alpha \stackrel{?}{=} Nv(4\pi\kappa/\lambda)$ which has been used to obtain values of κ from the value of $K = 2\alpha$ determined as above.

BIBLIOGRAPHY

[1]Kubelka, P., and F. Munk, 1931: "Reflection Characteristics of Paints", Z. Tech. Physik 12, p. 593.

[2]Reichman, J., 1973: "Determination of Absorption and Scattering Coefficients for Nonhomogeneous Media. 1: Theory", Appl. Optics 12, pp. 1811-1815.

[3]Van de Hulst, H.C., 1957: Light Scattering by Small Particles, John Wiley & Sons, Inc., New York, Chap. 9.

[4]Hansen, J.E., and L. D. Travis, 1974: "Light Scattering in Planetary Atmospheres", Space Science Reviews 16, pp. 527-610.

[5]Chandrasekhar, S., 1960: Radiative Transfer, Dover Publications, Inc., New York.

[6]Lindberg, J.D., and L.S. Laude, 1974: "Measurement of the absorption coefficient of atmospheric dust", Appl. Optics 13, pp. 1923-1927.

[7]Gillespie, J.B., J.D. Lindberg, and L.S. Laude, 1975: "Kubelka-Munk optical coefficients for a barium sulfate white reflectance standard", Appl. Optics 14, pp. 807-809.

[8]Lindberg, J.S., and J.B. Gillespie, 1976: private communication.

[9]Clark, Sydney P., Jr., ed., 1966: Handbook of Physical Constants, Memoir 97, The Geological Society of America, Inc., New York.

[10]Mudgett, P.S., and L.W. Richards, 1971: "Multiple Scattering Calculations for Technology", Appl. Optics 10, pp. 1485-1502.

[11]This calculation has been done by the author, but was not included in this report, inasmuch as it is purely manipulational. The crucial point is that the Wronskian $j_\ell(\rho)n'_\ell(\rho) - n_\ell(\rho)j'_\ell(\rho) = 1/\rho^2$, independent of ℓ.

[12]Schuster, A., 1905: Astrophys. J. 21, p. 1.

[13]Kortüm, G., 1969: Reflectance Spectroscopy, Springer-Verlag New York, Inc., Chap. IV.

[14]Van de Hulst, H.C., 1957: op. cit., Chap. 14, p. 270.

[15]Hansen, James E., 1971: "Multiple Scattering of Polarized Light in Planetary Atmospheres. Part II. Sunlight reflected by Terrestrial Water Clouds". J. Atmos. Sci. 28, pp. 1400-1426.

[16]Orchard, S.E., 1967: Astrophys. J. 149, 665.

[17]Gomez, R.B., C. Petracca, C. Querfeld, and G. Hoidale, 1975: "Atmospheric Effects for Target Signature Modeling. III: Discussion and Application of the ASL Scattering Model", Tech. Report ECOM-5558.

[18]Dave, J.V., 1969: Appl. Optics 8, 155.

[19]Kattawar, G.W., and G.N. Plass, 1967: Appl. Optics 6, 1377.

APPENDIX A

RADIATIVE TRANSFER THEORY AND NEAR FIELD PHASE FUNCTIONS

Imagine a beam of radiation incident at some angle θ_o with respect to the normal to the plane surface of a homogeneous random scattering medium. If the beam has a cross-section broad enough to subtend a very large number of particles in the medium, then, for purposes of analysis, the actual collection of particles of different optical types and sizes may be replaced by a collection of identical "average" particles, as follows.

Define: $N \equiv$ total number density; N_i = number density of type i particles; $f_i(r)dr$ = fraction of type i particles with radii in (r, r+dr), $\int dr\ f_i(r) = 1$; $\sigma_i(r,\underset{\sim}{s},\underset{\sim}{s}')$ = differential scattering cross-section of a particle of radius r, type i, from direction $\underset{\sim}{s}'$ to $\underset{\sim}{s}$; $\sigma^i_{ext}(r)$, $\sigma^i_{sca}(r)$, $\sigma^i_{abs}(r) \equiv$ (extinction, scattering, absorption) cross-sections of such a particle. Then the average particle has the following differential, extinction, scattering, and absorption cross-sections:

$$\sigma(\underset{\sim}{s},\underset{\sim}{s}') \equiv N^{-1} \sum_i N_i \int dr\ f_i(r)\sigma_i(r,\underset{\sim}{s},\underset{\sim}{s}')$$

$$\sigma_{ext,sca,abs} \equiv N^{-1} \sum_i N_i \int dr\ f_i(r)\sigma^i(r)\Big|_{ext,sca,abs.} \qquad \text{(A1)}$$

Here and in what follows, $\underset{\sim}{s}$, $\underset{\sim}{s}'$ are unit vectors. Imagine the medium divided into identical cubical cells, with side length equal to the average interparticle spacing ℓ, with $\ell^3 = 1/N$. Each cell contains one average particle, on the average, located randomly within the cell. As

long as the randomness in particle location extends over a wavelength or more, radiation intensities may be used, rather than phase-sensitive amplitudes.

Consider the cell with center at position $\underset{\sim}{x}$, and radiation on this cell in direction $\underset{\sim}{s}$ in $d\Omega_s$. The orientation of a cell is immaterial, so it may be chosen with two of its faces perpendicular to $\underset{\sim}{s}$, for any $\underset{\sim}{s}$. Therefore, the incident power on the cell is

$$P_{in}\, d\Omega_s = \ell^2\, I(\underset{\sim}{x}-\ell\underset{\sim}{s}/2,\underset{\sim}{s})d\Omega_s, \tag{A2}$$

where $I(\underset{\sim}{x}-\ell\underset{\sim}{s}/2)$ is the intensity on the incident cell face, which has a normal parallel to $\underset{\sim}{s}$, and a center at $\underset{\sim}{x} - \ell\underset{\sim}{s}/2$. This beam encounters the average particle somewhere in the cell, and scatters and absorbs radiation. The power lost out of $d\Omega_s$ is thus

$$P_{ext}\, d\Omega_s = \sigma_{ext}\, I\,(\underset{\sim}{x}-\ell\underset{\sim}{s}/2)d\Omega_s. \tag{A3}$$

On the other hand, part of the power from incident beams in all other directions gets scattered into $d\Omega_s$ by the particle; this power is

$$P_{sca}\, d\Omega_s = d\Omega_s \int d\Omega_s', \sigma(\underset{\sim}{s},\underset{\sim}{s}')I(\underset{\sim}{x}-\ell\underset{\sim}{s}'/2,\underset{\sim}{s}') \tag{A4}$$

where $I(\underset{\sim}{x}-\ell\underset{\sim}{s}'/2)$ is the intensity at an incident cell face, with center at $\underset{\sim}{x}-\ell\underset{\sim}{s}'/2$, normal parallel to $\underset{\sim}{s}'$. If $P_{out}\, d\Omega_s$ designates the power emerging from the cell in $d\Omega_s$, through the exit face centered at $\underset{\sim}{x} + \ell\underset{\sim}{s}/2$, then

$$P_{out}\, d\Omega_s = \ell^2\, I(\underset{\sim}{x}+\ell\underset{\sim}{s}/2,\underset{\sim}{s})d\Omega_s. \tag{A5}$$

Energy balance requires $P_{out} = P_{in} - P_{ext} + P_{sca}$, or

$$I(\underset{\sim}{x}+\ell\underset{\sim}{s}/2,\underset{\sim}{s}) = (1-\gamma\ell)I(\underset{\sim}{x}-\ell\underset{\sim}{s}/2)+\gamma\ell(4\pi)^{-1}\int d\Omega_{s'}\, p(\underset{\sim}{s},\underset{\sim}{s}')I(\underset{\sim}{x}-\ell\underset{\sim}{s}'/2,\underset{\sim}{s}'), \quad (A6)$$

where

$$\gamma \equiv N\sigma_{ext} = \text{extinction coefficient} \quad (A7)$$

$$p(\underset{\sim}{s},\underset{\sim}{s}') = (4\pi)\sigma(\underset{\sim}{s},\underset{\sim}{s}')/\sigma_{ext} \equiv \text{phase function.} \quad (A8)$$

Remember, $\ell^3 = N^{-1}$. Now make a Taylor expansion about the point $\underset{\sim}{x}$. If the change in I over distance $\ell/2$ is small, (which will be the case if $\gamma\ell << 1$), then terms proportional to $\gamma\ell|\underset{\sim}{\nabla}_x I|$ may be neglected, and Eq. A6 reduces to the standard radiative transfer (RT) equation[5],

$$\gamma^{-1}\underset{\sim}{s}\cdot\underset{\sim}{\nabla}_x I(\underset{\sim}{x},\underset{\sim}{s}) = -I(\underset{\sim}{x},\underset{\sim}{s})+(4\pi)^{-1}\int d\Omega_{s'}\, p(\underset{\sim}{s},\underset{\sim}{s}')I(\underset{\sim}{x},\underset{\sim}{s}'). \quad (A9)$$

The quantities (α,β), the (absorption, scattering) coefficients, are defined by

$$\alpha \equiv N\sigma_{abs}, \quad \beta = N\sigma_{sca}. \quad (A10)$$

Note that $\gamma = \alpha+\beta$, and that the phase function is normalized so that

$$(4\pi)^{-1}\int d\Omega_{s}\, p(\underset{\sim}{s},\underset{\sim}{s}') = N\sigma_{sca}/N\sigma_{ext} = \beta/\gamma \equiv \omega_o, \quad (A11)$$

the (single scattering) albedo.

This method of derivation makes it clear just how the scattering properties of the individual particles in a random mixture enter into the radiative transfer equation.

An interesting point arises for close-packed media, where a cell

is not much bigger than the average scattering particle. The above method of derivation makes it clear that the scatterer in the next cell (in direction $\underset{\sim}{s}$) sees the near zone and/or induction zone fields, rather than the radiation zone fields, from the scatterer in the given cell. Randomness of scatterer location extending over distances $\gtrsim \lambda$ still allows use of intensities rather than phase-sensitive quantities, but $\sigma(\underset{\sim}{s},\underset{\sim}{s}')$ should be replaced by $\sigma_{near}(\underset{\sim}{s},\underset{\sim}{s}')$ in the expression for P_{sca}, where $\sigma_{near}(\underset{\sim}{s},\underset{\sim}{s}')$ is a suitable near-field cross-section.

In this work, $\sigma_{near}(\underset{\sim}{s},\underset{\sim}{s}')$ was defined as follows. Consider the Mie scattering problem, with a spherical scatterer centered at the origin of coordinates, and a plane electromagnetic wave of unit power/unit area incident in direction $\underset{\sim}{s}'$. Let $\bar{\underset{\sim}{S}}(x,\hat{x},s') \equiv$ time-averaged Poynting vector of the scattered fields at distance x in direction $\hat{x}$. Then

$$\bar{\underset{\sim}{S}}(x,\hat{\underset{\sim}{x}},\underset{\sim}{s}') = \frac{c}{4\pi} \overline{\underset{\sim}{E}_{sca}(x,t) \times \underset{\sim}{B}_{sca}(\underset{\sim}{x},t)}.$$

The near field scattering cross-section is defined in this work by

$$\sigma_{near}(\underset{\sim}{s},\underset{\sim}{s}')d\Omega_s \equiv x^2 \, \underset{\sim}{s}\cdot\bar{\underset{\sim}{S}}(x,\underset{\sim}{s},\underset{\sim}{s}')d\Omega_s. \tag{A12}$$

Note that as $x \to \infty$, $\sigma_{near}(\underset{\sim}{s},\underset{\sim}{s}') \to \sigma(\underset{\sim}{s},\underset{\sim}{s}')$, the usual differential cross-section defined in terms of the asymptotic fields. The distance x was taken to be equal to some factor times the particle radius r, for each particle in a mixture, in this work. Explicitly, σ_{near} was defined by

$$\sigma_{near}(\underset{\sim}{s},\underset{\sim}{s}') \equiv N^{-1} \sum_i N_i \int dr \, f_i(r)\sigma_i(Fr;r,\underset{\sim}{s},\underset{\sim}{s}'); \tag{A13}$$

that is, the fields used in evaluating the cross-section of a particle of radius r are those at a distance Fr from the particle's center, since these are approximately the ones incident on the neighboring particles. If $N = 1/\ell^3$ is the overall number density, $v \equiv N^{-1}\sum_i N_i v_i$ is the volume of an average particle, then the factor F should be chosen as

$$F = (\ell^3/v)^{1/3} = (1/Nv)^{1/3} . \tag{A14}$$

Note that $F > 1$ as long as there are air spaces between particles, which there must be if the medium is to be a random scattering medium.

It is straightforward but nontrivial[11] to show that the above definition of the near field cross-section yields

$$\int_{4\pi} \sigma_{near}(\underset{\sim}{s},\underset{\sim}{s}')d\Omega_s = \sigma_{sca}, \tag{A15}$$

where σ_{sca} is the conventional asymptotic total scattering cross-section, independent of x. Since any absorption by the scatterer is strictly localized to regions within the scatterer, conservation of energy shows that $\sigma_{ext}^{(near)} = \sigma_{sca} + \sigma_{abs} = \sigma_{ext}$, also independent of x. Define the near-field phase function by

$$p_{near}(\underset{\sim}{s},\underset{\sim}{s}') \equiv 4\pi\, N\sigma_{near}(\underset{\sim}{s},\underset{\sim}{s}')/\gamma,\ (4\pi)^{-1}\int_{4\pi} d\Omega_s\ p_{near}(\underset{\sim}{s},\underset{\sim}{s}') = \omega_o. \tag{A16}$$

This phase function has a different angular dependence than the far field one, although its normalization is the same. An appropriate radiative transfer equation for close-packed random scattering media is then

$$\gamma^{-1}\ \underset{\sim}{s}\cdot\underset{\sim}{\nabla}I(\underset{\sim}{x},\underset{\sim}{s}) = -I(\underset{\sim}{x},\underset{\sim}{s}) + (4\pi)^{-1}\int d\Omega_{s'}\ p_{near}(\underset{\sim}{s},\underset{\sim}{s}')I(\underset{\sim}{x},\underset{\sim}{s}'), \qquad \text{(A17)}$$

as long as $\gamma\ell << 1$. If $\gamma\ell \lesssim 1$, a simple differential equation cannot be obtained from Eq. (A6); this case is considered in appendices E and I.

For problems with (xy)-translation invariance, which are the only ones treated in this work, Eqs. A9 and A17 reduce to the form

$$\mu\frac{\partial I}{\partial t}(z,\mu,\phi) = -\gamma I(z,\mu,\phi) + \frac{\gamma}{4\pi}\int_{-1}^{1} d\mu'\int_{o}^{2\pi} d\phi'\ p(\mu,\phi,\mu',\phi')I(z,\mu',\phi'), \qquad \text{(A18)}$$

where ($\phi=\cos^{-1}\mu,\phi$) are the polar angles of the unit vector $\underset{\sim}{s}$ with respect to the z-direction. Since only total fluxes (transmitted and reflected) are of interest in this work, the relevant radiative transfer equation is obtained by integrating Eq. (A18) over all azimuth angles ϕ.

Define

$$I(z,\mu) \equiv (2\pi)^{-1}\int_{o}^{2\pi} d\phi\ I(z,\mu,\phi);\ p^{(o)}(\mu,\mu') \equiv (2\pi)^{-1}\int_{o}^{2\pi} d\phi\ p(\mu,\phi,\mu',\phi'). \qquad \text{(A19)}$$

Then Eq. (A18) reduces to

$$\mu\frac{\partial I}{\partial z}(z,\mu) = -\gamma I(z,\mu) + \frac{1}{2}\gamma\int_{-1}^{1} d\mu'\ p^{(o)}(\mu,\mu')I(z,\mu') \qquad \text{(A20)}$$

which is the standard azimuth-independent radiative transfer equation for problems with (xy)-translational invariance. Here, $p^{(o)}(\mu,\mu')$ is formed from either the near field or far field phase functions discussed above.

If there is a uniform incident beam, such that $I_{in}(0,\mu,\phi) = \pi F\delta(\mu-\mu_o)\delta(\phi-\phi_o)$, then $I_{in}(0,\mu) = \frac{1}{2} F\delta(\mu-\mu_o)$, and $I_{in}(z,\mu) = \frac{1}{2} F\delta(\mu-\mu_o)e^{-\gamma z/\mu}$. Substituting this into (A20), with $I(z,\mu) = I_{in}(z,\mu) + I_{di}(z,\mu)$, yields

$$\mu \frac{\partial I_{di}}{\partial z} = -\gamma I_{di}(z,\mu) + \frac{1}{2}\gamma\int_{-1}^{1} d\mu' \; p^{(o)}(\mu,\mu')I_{di}(z,\mu') + \frac{\gamma}{4} F \, p^{(o)}(\mu,\mu_o)e^{-\gamma z/\mu_o}, \tag{A21}$$

which is the relevant radiative transfer equation for the diffuse intensity $I_{di}(z,\mu)$. It is this equation which was solved accurately, using computer algorithms based on the doubling method of Van de Hulst and Hansen, for media of various thicknesses d (optical thickness $\tau = \gamma d$). Both near and far field phase functions were used and compared.

APPENDIX B

KUBELKA-MUNK THEORY

The Kubelka-Munk (KM) theory[1] is equivalent to the Schuster two-flux theory[12] of radiation transfer in plane parallel homogeneous random scattering media. In Eq. (A20), assume that

$$I(z,\mu) = I_+(z),\ \mu > 0;\ I(z,\mu) = I_-(z),\ \mu < 0$$

and integrate Eq. (A20) over $0 \le \mu \le 1$, and over $0 \ge \mu \ge -1$. This yields the KM equations

$$\begin{aligned} \frac{d\Phi_+}{dz} &= -(K+S)\Phi_+ + S\Phi_- \\ \frac{d\Phi_-}{dz} &= (K+S)\Phi_- - S\Phi_+ \end{aligned} \tag{B1}$$

where $K \equiv 2\alpha$, $S \equiv 2\beta_-$; $\beta_\pm \equiv \frac{\gamma}{2}\int_o^1 d\mu \int_o^1 d\mu'\ p^{(o)}(\mu,\pm\mu')$; $\Phi_\pm \equiv \int_o^1 d\mu\ \mu\ I_\pm(z) = \frac{1}{2} I_\pm$ = (magnitude of) fluxes; and $\gamma = \alpha+\beta_+ + \beta_-$. Note that S is twice the back-scattering coefficient, and K is twice the absorption coefficient, just as in the usual *ad hoc* derivation of the KM equations[13]. In this work, the sample had thickness d, and was placed on a black background of reflectance $R_g \equiv 0$. The solution of Eqs. (B1), subject to the boundary conditions $(\Phi_-/\Phi_+)_{z=o} = R_d$, $(\Phi_-/\Phi_+)_{z=d} = R_g = 0$, yields the KM relations

$$\frac{K}{S} = \frac{(1-R_\infty)^2}{2R_\infty}\ ,\ Sd = \frac{R_\infty}{1-R_\infty^2}\ \ell n\left(\frac{1-R_dR_\infty}{1-R_d/R_\infty}\right)\ , \tag{B2}$$

where R_∞ is the reflectance of an infinitely thick sample. These relations

have often been used to evaluate K, S, from measured values of R_d, R_∞.

In the usual ad hoc derivation of the KM theory[13], the incident illumination is supposed to be either diffuse and isotropic, or a beam at $\theta_o = 60°$ ($\mu_o = 1/2$).

Note well that the two-flux approximation to the full RT Eq. (A20) is very crude, and that all directional effects which would be caused by beam incidence at an arbitrary angle θ_o, rather than by diffuse isotropic incidence, are lost.

APPENDIX C

REICHMAN THEORY

This two-flux theory, developed by Reichman[2], starts from Eq. (A21) rather than (A20), so it represents an attempt to include incident beam directional effects. In Eq. (A21), assume that

$$I_{di}(z,\mu) = I_+(z),\ \mu>0;\ I_{di}(z,\mu) = I_-(z),\ \mu<0;\ F = 1;$$

and integrate Eq. (A10) over $0\le\mu\le1$, and over $0\ge\mu\ge -1$. This yields

$$\begin{aligned}\frac{d\Phi_+}{dz} &= -(K+S)\Phi_+ + S\Phi_- + \gamma P_+(\mu_o)e^{-\gamma z/\mu_o}\\ \frac{d\Phi_-}{dz} &= (K+S)\Phi_- - S\Phi_+ - \gamma P_-(\mu_o)e^{-\gamma z/\mu_o}\end{aligned} \tag{C1}$$

where $K \equiv 2\alpha$, $S \equiv 2\beta_-$, $\Phi_\pm = I_\pm/2$, just as in Appendix B; and

$$P_\pm(\mu_o) \equiv \frac{1}{4}\int_o^1 d\mu\ p^{(o)}(\mu,\pm\mu_o). \tag{C2}$$

Equations (C1) are very similar to the KM equations (B1), except that here, $\Phi_\pm$ are diffuse fluxes only; the incident flux is $\Phi_{in}(z) = \int_o^1 d\mu\ \mu\ \frac{1}{2}\ \delta(\mu-\mu_o)e^{-\gamma z/\mu} = \frac{\mu_o}{2}\ e^{-\gamma z/\mu_o}$. Boundary conditions are $\Phi_-(d) = 0$ (black background), $\Phi_+(0) = 0$. The reflectance is $R_d \equiv \Phi_-(0)/\Phi_{in}(0)$ for a sample of thickness d.

In general, the solution of these equations with these boundary conditions yields

$$R_d = \frac{2}{\mu_o}\left\{D_- - \frac{SD_+\sinh(Ld) + LD_- \exp-\gamma d/\mu_o}{(K+S)\cosh(Ld) + L\sinh(Ld)}\right\} \qquad (C3)$$

where $L^2 \equiv K^2 + 2KS$, and $D_\pm \equiv \gamma[(K+S \pm \gamma/\mu_o)P_\pm + SP_\mp]/(L^2-\gamma^2/\mu_o^2)$.

In the special case that $\mu_o = \frac{1}{2}$ (angle of incidence = 60°) and $\beta_+ = \beta_- = \frac{\beta}{2}$, $P_+ = P_- = \omega_o/4$, (isotropic scatterers will yield this), Eqs. (C3) yield just the KM relations (B2) for K/S and Sd in terms of R_d and R_∞. In all other cases, the expressions for K/S and Sd are different.

This means that the original KM theory should be just as good an approximation as this modified theory if $\theta_o = 60°$, and if the scattering is isotropic; but that the KM theory should be less accurate than this modified theory for beam incidence at other angles, and/or for non-isotropic phase functions.

In this work, the predictions of R_d, R_∞ from this modified theory wave checked against those from the accurate doubling method solutions of the RT equations, and were found to agree within 15% for all samples which were modelled. Similar agreement has been noted by Reichman[2]. Equations (C3) may be rewritten in the following form, with $\exp(-\gamma d/\mu_o) \approx 0$:

$$R_d \approx \frac{8R_K(2R_K\Gamma a_+ - a_-)}{(1+R_K)^2 - 4\mu_o^2(1-R_K)^2} \quad , \qquad (C4)$$

where $K/S \equiv (1-R_K)^2/2R_K$; $a_\pm \equiv P_+(\mu_o)[(1 + K/S)\mu_o \pm (1 + K/2S)] + \mu_o P_-(\mu_o)$, $\Gamma \equiv (1 - e^{-2Ld})/(1 + R_K^2\, e^{-2Ld})$.

For samples of optical thickness $\gamma d \gtrsim 4$, this is a very good approximation. In principle, measurement at a given μ_o of R_∞ and R_d at three

other d, will allow inversion of Eq. (C4) to obtain values of the four unknowns R_κ, L, a_+, a_-. In turn, knowledge of these four quantities allows determination of the Mie theory parameters $(\alpha,\beta_\pm,\gamma)$, or, since N is known, the cross-sections σ_{abs}, σ_{sca}, σ_{ext} for the average particle in the medium. If the particle types, number densities, and size distributions are known reasonably well, Mie theory computer algorithms could be used to zero in on values of the real and imaginary refractive indices of each type of particle in the medium. This possibility was not pursued in this work, but it seems to merit further study.

APPENDIX D

RELATION BETWEEN κ AND α

Consider a random scattering medium composed of N particles/unit volume. For convenience in what follows, let all the particles have the same radius, r, volume $v = 4\pi r^3/3$, and the same refractive index, $m = n - i\kappa$; the discussion presented below can be extended trivially to include the general case.

As long as the arrangement of particles is homogeneous, but the randomness in the location of each particle is greater than a wavelength, λ, the conditions for applicability of the standard radiative transfer equations (A9) are met, and the absorption coefficient, α, of the medium is defined in terms of the Mie theory absorption cross-section, σ_{abs}, by

$$\alpha \equiv N\sigma_{abs}. \tag{D1}$$

The derivation of the KM equations in Appendix B, and the Reichman equations, in Appendix C, makes it clear that the KM absorption coefficient K is defined by $K = 2\alpha$.

Now imagine that this collection of particles is fused, with the particles distorted as necessary and assembled so that there are no longer any air spaces between them. Then this collection of particles is indeed a uniform material medium, possessing as a whole a refractive index $m = n - i\kappa$. The absorption coefficient = extinction coefficient of this medium is obviously

$$\alpha_m = 4\pi\kappa/\lambda. \tag{D2}$$

This follows from the behavior of a plane wave exp $i(\omega t - 2\pi m\, z/\lambda)$ traveling in any direction, say, the z-direction.

In some work, the plausible hypothesis has been made that α_m should be related to α simply by the ratio of the total volume occupied by the random scattering medium to that occupied by the same total number of particles arranged as a uniform material medium.[6,7,8] That is, the hypothesis is

$$\alpha \stackrel{?}{=} Nv\, \alpha_m = Nv(4\pi\kappa/\lambda). \qquad \text{(D3)}$$

That this hypothesis is plausible follows from the reasoning that the amount of energy absorbed by a particle should be proportional to its volume, for a given incident radiation field. However, it is clear that the absorption by a volume element of a substance is proportional to the local intensity inside that volume element, not to the incident intensity on the element. If the (average) particles in a random scattering medium are compressed so tightly that the medium becomes a true material medium (no boundaries, no diffuse scattering), then the local intensity in each volume element which was subtended by a given particle is completely different from the local intensity which existed inside the corresponding volume element in the random scattering medium. In going from scattering medium to material medium, local intensity is not invariant, which it would have to be in order that the hypothesis be valid. Note that it is the single-scattering local intensity that is considered here, because the absorption coefficient

of a random scattering medium is defined in terms of a layer of particles so thin that multiple scattering in that layer may be neglected. Therefore, the question of whether the local intensity changes can be answered by single scattering theory, e.g., Mie theory for the spherical particles considered in this work.

Combining Eq. (D1) and the hypothesis, Eq. (D3), yields the equivalent hypothetical relation

$$\sigma_{abs} \stackrel{?}{=} 4\pi\kappa v/\lambda. \tag{D4}$$

This hypothetical relation is expressed entirely in terms of Mie theory parameters, and may be checked by that theory alone. Several examples will serve to show that the hypothesis is valid only for small particles whose refractive index is close to 1, and badly violated for other cases.

Van de Hulst[14] gives the following approximate expression for σ_{abs}, valid for $(2\pi r/\lambda)^2 \ll 1$, for any m, for a particle of radius r:

$$\sigma_{abs} = -\mathrm{Im}\left\{\pi r^2\left[\frac{8\pi r}{\lambda}\frac{m^2-1}{m^2+2} + \frac{4}{15}\left(\frac{2\pi r}{\lambda}\right)^3\left(\frac{m^2-1}{m^2+2}\right)^2\left(\frac{m^4+27m^2+38}{2m^2+3}\right) + O\left(\frac{2\pi r}{\lambda}\right)^4\right]\right\}. \tag{D5}$$

case i) $(2\pi r/\lambda)^2 << 1$, $n \simeq 1$, $\kappa << 1$. Then only the first term in Eq. (D5) contributes; $\mathrm{Im}((n^2-1)/m^2+2) = -2\kappa/3$, and $\sigma_{abs} = (4\pi r^3/3)(4\pi/\lambda)\kappa = 4\pi\kappa v/\lambda$, in agreement with the hypothesis, Eq. (D4).

case ii) $(2\pi r/\lambda)^2 \lesssim 1$, $n = 2$, $\kappa << 1$. Then Eq. (D5) yields, after some arithmetic,

$$\sigma_{abs} \approx (4\pi\kappa v/\lambda)\left(\frac{1}{2} + \frac{9}{16}(2\pi r/\lambda)^2\right). \qquad \text{(D6)}$$

It is seen that, if $(2\pi r/\lambda) << 1$, the hypothesis, Eq. (D4), is violated by a factor of 2; that is, using Eq. (D4) and an experimentally determined $\sigma_{abs} = \alpha/N$, one would predict a value of κ only half as large as the actual value. For $(2\pi r/\lambda) \simeq 1$, Eq. (D6) seems to agree with the hypothesis, but the neglected terms of $O(2\pi r/\lambda)^4$ and higher in Eq. (D5) make Eq. (D6) invalid for $(2\pi r/\lambda) \simeq 1$.

The general case, with both $2\pi r/\lambda$ and m allowed to have any reasonable values, cannot be analyzed except by use of the full Mie theory. For example, in the limiting case of very large scatterers $(2\pi r/\lambda >> 1)$, the asymptotic relation from Mie theory is

$$\sigma_{abs} = \pi r^2(1-\omega_o) = v\frac{3}{4r}(1-\omega_o), \quad 0 \leq \omega_o \leq 1. \qquad \text{(D7)}$$

The hypothesis, Eq. (D4), would thus require

$$16\pi r/3\lambda \stackrel{?}{=} (1-\omega_o),$$

which is clearly very badly violated for $2\pi r/\lambda >> 1$.

Standard Mie theory computer algorithms, such as those used in this work, can accurately and easily predict values for σ_{abs}, σ_{sca}, σ_{ext}, ...,

at any λ, given i) the optical constants (n_i, κ_i) of the type i particles in the medium to be modelled, and ii) the size distribution $f_i(r)$ of each type of particle. Unfortunately, it is not so easy to invert these calculations, not even in the simplest case of a monodisperse collection of one optical type of particle. In this simplest case, for example, suppose the real refractive index, n, is known, and the radius r is known, for a constituent particle. If there is at least an order-of-magnitude feeling for what the value of the imaginary index κ ought to be, then the standard computer algorithms can be used to search around the expected value of κ until that value is found which reproduces the experimentally determined σ_{abs}. But this kind of search increases immensely in complexity as the structure of the medium increases. In order to use this method practically, it would be necessary to know the n_i, $f_i(r)$ for all the types of particles in the mixture to be modelled, as well as the κ_i for all the types but the one of interest, which is the value that this method would be attempting to determine. Alternatively, and much more simply, one could perhaps experimentally determine the $\sigma_{abs}^{(i)}$ separately for all the constituents of a mixture, and then the σ_{abs} for the mixture. From (A1), then, for an n-component mixture,

$$N_i \int dr\, f_i(r)\, \sigma_{abs}^{(i)}(r) = N\sigma_{abs} - \sum_{j \neq i}^{n} N_j \sigma_{abs}^{(j)} = N_i \sigma_{abs}^{(i)} \,. \qquad (D8)$$

This equation has a known value of $\alpha_i = N_i \sigma_{abs}^{(i)}$ only if i) it was directly measured by determining α_i in a single-component medium (usually not practicable), or ii) the values of σ_{abs} and $\sigma_{abs}^{(j)}$, $j \neq i$, were determined experimentally by determining α and α_j, and the same size distributions

were kept for all components throughout. Then, if $f_i(r)$ and n_i are known reasonably well, and κ_i is known within order-of-magnitude, the Mie theory algorithms could be operated in the above search mode to determine κ_i. For example, suppose the diffuse reflectance experimental test uses a sample which is a mixture of barium sulphate and just one other component, say, carbon. Imagine that σ_{abs} (carbon) could not be found directly by experiment. Then the first equality in Eq. (D8) would be used. Now, if component number 1 is carbon, number 2 is barium sulphate, and if $\alpha_2 = N_2\,\sigma_{abs}^{(2)}$ and $\alpha = N\sigma_{abs}$ for the mixture have been determined by reflectance experiments, then, from Eq. (D8)

$$\sigma_{abs}^{(1)} = \int dr\; f_i(r)\; \sigma_{abs}^{(1)}(r) = (N_1)^{-1}[N\sigma_{abs} - N_2\sigma_{abs}^{(2)}] \;, \tag{D9}$$

and the search mode could be used with this relation, to determine κ for carbon, provided f(r), n, and N for the carbon in this mixture were quite well known. If all the carbon particles had $(2\pi r/\lambda) << 1$, then the first term on the RHS of Eq. (D5) could be used, weighted with $f_1(r)$:

$$\sigma_{abs}^{(1)} = -\frac{6\pi v_1}{\lambda}\,\mathrm{Im}\left(\frac{m^2-1}{m^2+2}\right) \;, \tag{D10}$$

where $v_1 \equiv \int dr f_1(r) 4\pi r^3/3$. This can be solved easily for κ, if n and v_1 are known.

APPENDIX E

RADIATIVE TRANSFER THEORY IN ONE DIMENSION

This section is included because it illustrates simply and clearly three very important fundamental points: i) the connection between imaginary refractive index and absorption cross-section, ii) the transition from wave theory to radiative transfer theory, iii) the correct difference rather than differential equations of radiative transfer theory.

Let the stretched string be the one-dimensional physical system which supports wave motion. Consider first a uniform string of mass/unit length μ, under tension τ. This string supports transverse oscillations $u(x,t)$ which obey the wave equation

$$\mu \frac{\partial^2 u}{\partial t^2} = \tau \frac{\partial^2 u}{\partial x^2} , \tag{E1}$$

and which have fundamental solutions $u(x,t)$ at a given frequency ω:

$$u(x,t) = e^{i\omega t}(A_+ e^{-ikx} + A_- e^{ikx}), \; k \equiv \omega/c, \; c^2 \equiv \tau/\mu, \tag{E2}$$

where $A_\pm$ are undetermined complex-valued amplitudes.

Consider another string, also under tension τ, but with mass/unit length μ_1, with oscillations which satisfy

$$\mu_1 \frac{\partial^2 u}{\partial t^2} + \sqrt{\mu_1 \tau}\, \gamma \frac{\partial u}{\partial t} = \tau \frac{\partial^2 u}{\partial x^2} . \tag{E3}$$

Here, the term $\sqrt{\mu_1 \tau}\, \gamma \, \partial u/\partial t$ is a frictional term, representing absorption. The fundamental solutions $u(x,t)$ at frequency ω are

$$u(x,t) = e^{i\omega t}(A_+ e^{-imkx} + A_- e^{imkx}),\ k = \omega/c, \tag{E4}$$

with $m \equiv \sqrt{\eta - i\gamma\eta/k} \equiv n - i\kappa$, $\kappa > 0$, $\eta \equiv \sqrt{\mu_1/\mu}$. These choices of sign ensure that a traveling wave is damped in its direction of travel. A wave traveling in the positive x-direction has the form

$$e^{i\omega t}\ e^{-inkx}\ e^{-2\pi\kappa x/\lambda} \tag{E5}$$

which shows that the wavespeed on this string is c/n, and the extinction coefficient is $4\pi\kappa/\lambda$. For small γ, ($\gamma\eta/k << 1$), $n \simeq \eta$, and $4\pi\kappa/\lambda \simeq \gamma$.

1. Single Scattering

Now imagine a piece of the frictional string of length r, inserted between infinitely long segments of the original frictionless string. This situation is exactly analogous to that of a particle of radius r, refractive index m, in vacuum. Let a wave $u_1(x,t) = A_1^+\ e^{i\omega t}\ e^{-ikx}$ be incident from the left on the segment, and a wave $A_2^-\ e^{i\omega t}\ e^{ikx}$ be incident from the right. Boundary conditions are continuity of u and $\partial u/\partial x$ at each interface. Application of these boundary conditions yields the matrix relations

$$\begin{pmatrix} A_2^+ \\ A_2^- \end{pmatrix} = (M)\begin{pmatrix} A_1^+ \\ A_1^- \end{pmatrix} \tag{E6}$$

where A_2^+ is the complex amplitude of the right-traveling wave just to the right of the segment, and A_1^- is the complex amplitude of the left-traveling wave just to the left of the segment. The matrix M is

$$(M) = \frac{1}{4m}\begin{pmatrix} 1+m & 1-m \\ 1-m & 1+m \end{pmatrix}\begin{pmatrix} e^{-ikmr} & 0 \\ 0 & e^{ikmr} \end{pmatrix}\begin{pmatrix} m+1 & m-1 \\ m-1 & m+1 \end{pmatrix} \tag{E7}$$

Note that

$$\det(M) = 1. \tag{E8}$$

Consider the case $A_2^- \equiv 0$ (no wave incident from the right). Then Eq. (E6) yields

$$\begin{aligned} R &\equiv |A_1^-|^2/|A_1^+|^2 = |M_{21}|^2/|M_{22}|^2 = \text{reflection coefficient} \\ T &\equiv |A_2^+|^2/|A_1^+|^2 = 1/|M_{22}|^2 = \text{transmission coefficient} \end{aligned} \tag{E9}$$

R is the fraction of the incident power which is reflected; T, the fraction which is transmitted. If m is real, R+T = 1; since m is complex, the quantity

$$A \equiv 1 - (R+T) \tag{E10}$$

is the fraction of the incident power which is absorbed. This absorption fraction A is the analog of the absorption cross-section of a scattering particle in 3 dimensions. For the case $\kappa \ll 1$, $2\pi r/\lambda \ll 1$, but n arbitrary, the above equations yield

$$A = (4\pi\kappa r/\lambda)(n). \tag{E11}$$

For n=1, this is the exact analog of the hypothesis, (Eq. D4), $\sigma_{abs} = 4\pi\kappa v/\lambda$, in three dimensions. Here, just as in three dimensions, such a hypothesis is badly violated in general.

2. Transition to Radiative Transfer Theory

Consider a collection of the absorbing segments described above, inserted at random intervals, with no overlap, in the original frictionless string. The distribution of these segments is to be homogeneous, which means that there exists an average intersegment spacing, ℓ, and thereby an average number of segments per unit length, $N \equiv 1/\ell$.

Consider the n^{th} segment. Let (A_n^+, A_{n+1}^-) be the complex amplitudes of the waves incident on this segment from the (left, right), respectively, and (A_n^-, A_{n+1}^+) be the complex amplitudes of the waves traveling away from (scattered by) the segment on the (left, right), respectively. These amplitudes are related by the matrix M, as in Eq. (E6). Solution of Eq. (E6) for (A_{n+1}^+, A_n^-) in terms of (A_n^+, A_{n+1}^-) yields

$$\begin{pmatrix} A_{n+1}^+ \\ A_n^- \end{pmatrix} = \frac{1}{M_{22}} \begin{pmatrix} 1 & M_{21} \\ -M_{21} & 1 \end{pmatrix} \begin{pmatrix} A_n^+ \\ A_{n+1}^- \end{pmatrix} , \tag{E12}$$

where the equality $M_{12} = -M_{21}$ has been used. These amplitudes $A_n^+, \ldots,$ are the amplitudes of the various waves at the appropriate interfaces between the n^{th} segment and the frictionless string.

The randomness in the segment placing means that there is zero correlation in phase between A_{n+1}^- and A_n^+. This means that $< A_{n+1}^- A_n^{+*} > = 0$, where $< \ >$ $\equiv$ expectation over all possible postions of all segments. Taking $<|A_{n+1}^+|^2> \equiv I_{n+1}^+$, $<|A_n^-|^2> \equiv I_n^-$, etc., and using Eqs. (E9), yields

$$I_{n+1}^+ = TI_n^+ + RI_{n+1}^-, \quad I_n^- = TI_{n+1}^- + RI_n^+ . \tag{E13a}$$

Solving these equations for the intensities $I^{\pm}_{n+1}$ yields

$$I^{+}_{n+1} - I^{+}_{n} = -(1-T+R^2/T)I^{+}_{n} + \frac{R}{T} I^{-}_{n} \approx -(1-T)I^{+}_{n} + RI^{-}_{n},$$

$$I^{-}_{n+1} - I^{-}_{n} = (\frac{1}{T} -1)I^{-}_{n} - \frac{R}{T} I^{+}_{n} \approx (1-T)I^{-}_{n} - RI^{+}_{n}, \tag{E13}$$

where the approximate equalities follow for R<<1, A<<1, T≤1. Here, the intensities I^{+}_{n+1}, I^{-}_{n+1} are the intensities of the wave disturbance at any point between the n^{th} and $(n+1)^{th}$ segment; similarly for I^{+}_{n}, I^{-}_{n}. This follows because the string is frictionless between segments. Therefore, if the medium is imagined to be divided into cells of length $\ell = N^{-1}$, with on the average one segment anywhere in each cell, the intensities $I^{\pm}_{n+1}$ can be taken as the intensities on the right cell boundary, while $I^{\pm}_{n}$ are those on the left cell boundary. Dividing both sides of Eqs. (E13) by ℓ, treating the case R<<1, A<<1 only, and making the transition $n\ell \to x$ = continuous variable, $I^{\pm}_{n} \to I_{\pm}(x)$, yields

$$\frac{dI_{+}}{dx} = -(K+S)I_{+} + SI_{-},$$

$$\frac{dI_{-}}{dx} = (K+S)I_{-} - SI_{+}, \tag{E14}$$

where

$$K \equiv NA, \quad S \equiv NR, \tag{E15}$$

are kept constant during the limiting process. These are radiative transfer theory equations for this model one-dimensional system. Note that they have the same form as the KM equations (B1), and that the significance of (K,S) is the same: In both, K = absorption/unit length,

S = back-scattering/unit length, in the medium, (except for a factor of two which is geometrical in origin).

However, for strongly absorbing or reflecting segments, the full equalities of Eqs. (E13) must be used. Letting $n\ell \to x$ = continuous variable, $I_n^{\pm} \equiv I_{\pm}(x)$, $I_{n+1}^{\pm} \equiv I_{\pm}(x+\ell)$, these equations reduce to

$$\begin{aligned} I_+(x+\ell) &= (1-a)I_+(x) + bI_-(x), \\ I_-(x+\ell) &= -bI_+(x) + (1+c)I_-(x), \end{aligned} \tag{E16}$$

where

$$a \equiv (T-T^2+R^2)/T,\ b \equiv R/T,\ c \equiv (1-T)/T. \tag{E17}$$

Equations (E16) are difference equations rather than differential equations. The desired physical solutions are the "smoothest" functions $I_{\pm}(x)$ which yield the correct $I_n^{\pm}$ on the points $x = n\ell$.

These equations may be solved by normal mode methods. Let $I_{\pm}(x) = A_{\pm}\, e^{px}$ in Eqs. (E14). This results in the eigenvalue equations

$$\begin{pmatrix} 1-a-e^{p\ell} & b \\ -b & 1+c-e^{p\ell} \end{pmatrix} \begin{pmatrix} A_+ \\ A_- \end{pmatrix} = 0 \tag{E18}$$

Solution of this for the eigenvalues $p_{1,2}$ and eigenvectors yields

$$p_{1,2} = \ell^{-1}\, \ell n(1+q_{1,2}),\ A_{-(1,2)} = b^{-1}(a+q_{1,2})A_{+(1,2)}, \tag{E19}$$

where

$$q_{1,2} = \frac{1}{2}(c-a) \pm \left[c-a + \frac{1}{4}(c-a)^2\right]^{1/2}. \tag{E20}$$

The fundamental solutions are the superposition of these normal modes:

$$I_+(x) = A_{+1}\, e^{p_1 x} + A_{+2}\, e^{p_2 x}$$

$$I_-(x) = b^{-1}[(a+q_1)A_{+1}\, e^{p_1 x} + (a+q_2)A_{+2}\, e^{p_2 x}]. \qquad \text{(E21)}$$

It is simple and straightforward to verify that these solutions satisfy (the first equalities) in Eqs. (E13), on the points $x = n\ell$.

It is worth noting that the general solution of Eqs. (E16) may be written

$$\bar{I}_+(x) = e^{p_1 x}\, f_1(x) + e^{p_2 x}\, f_2(x),$$

$$\bar{I}_-(x) = b^{-1}[(a+q_1)e^{p_1 x}\, f_1(x) + (a+q_2)e^{p_2 x}\, f_2(x)],$$

where $f_1(x)$, $f_2(x)$ are any two functions periodic in x with period ℓ. Since the desired physical solutions are to be the "smoothest" functions between the points $x = (n\ell, (n+1)\ell)$, it is necessary to choose $f_1(x) = A_{+1} = \text{const.}$, $f_2(x) = A_{+2} = \text{const.}$ The possible oscillations represented by non-constant $f_{1,2}(x)$ result from the extra (infinitely many) degrees of freedom introduced in going from the correct discrete equations (E13) to the continuous difference equations (E16); these extra degrees of freedom are clearly spurious.

It is instructive to note that, if the difference equations (E16) were first converted to differential equations by the standard method, using $\text{Lim}(\ell\to 0)[(I_+(x+\ell) - I_+(x))/\ell] \equiv dI_+/dx$, etc., and then solved, the results would have been

$$dI_+/dx = \ell^{-1}(-aI_+ + bI_-),\ dI_-/dx = \ell^{-1}(-bI_+ + cI_-), \qquad \text{(E22)}$$

with solutions

$$I_+(x) = A_{+1}\, e^{q_1 x/\ell} + A_{+2}\, e^{q_2 x/\ell}$$
$$I_-(x) = b^{-1}[(a+q_1)A_{+1}\, e^{q_1 x/\ell} + (a+q_2)A_{+2} e^{q_2 x/\ell}] \qquad \text{(E23)}$$

where $\mathrm{Lim}(\ell\to 0)[a/\ell,\ b/\ell,\ c/\ell] \equiv$ constants. Inspection of Eqs. (E19), (E21) shows that these expressions are the correct solutions only if $|q_{1,2}|<<1$, since then $p_{1,2} = \ell^{-1}\ \ell n(1+q_{1,2}) \simeq q_{1,2}/\ell$. That is to say, only if the changes in $I_\pm$ over one cell are small are the differential equations (E23) equivalent to the difference equations (E16). In order for these changes to be small, $|q_{1,2}|$ must be <<1. If both A<<1, R<<1, then the differential equations (E23) are indeed just the equations (E14). Note that $|q_{1,2}|<<1$ follows if only A<<1, regardless of R. If only A<<1, but R $\lesssim$ 1, the differential equations (E22) are correct, but they are not the same as the KM equations (E14). This point is made clear by an example in Appendix I.

The solutions (E21) of the difference equations (E16), subject to the boundary conditions analagous to those for a plane parallel sample of thickness d in 3-dimensions,

$$I_-(d) = 0,\ I_+(0) = 1 \qquad \text{(E24)}$$

yield the following expressions involving the reflectances R_d, R_∞:

$$R_\infty = (a+q_2)/b;\ (p_1-p_2)d = \ell n\left(\frac{1-R_d R_\infty}{1-R_d/R_\infty}\right) \qquad \text{(E25)}$$

where $R_d \equiv I_-(0)$ for a sample of total length d. In the limit A<<1, R<<1, these reduce exactly to the form of the KM relations (B2),

$$\frac{K}{S} = \frac{(1-R_\infty)^2}{2R_\infty}\ ,\ Sd = \frac{R_\infty}{1-R_\infty^2}\ \ell n\left(\frac{1-R_dR_\infty}{1-R_d/R_\infty}\right), \tag{E26}$$

where K,S are defined here by Eqs. (E15), with $N = \ell^{-1}$.

It is enlightening to contrast the two solutions by means of a numerical example. Consider strongly reflecting, moderately absorbing segments, with

$$A = 0.1,\ R = 0.8,\ T = 0.1. \tag{E27}$$

Then, from Eqs. (E17), (E19), (E20),

$$a = 7.3,\ b = 8,\ c = 9;\ q_{1,2} = 2.40,\ -0.70;$$

$$p_{1,2} = 1.22/\ell,\ -1.20/\ell. \tag{E28}$$

The correct relations, from Eq. (E25), are then

$$R_\infty = 0.825,\ \ell n\left(\frac{1-R_dR_\infty}{1-R_d/R_\infty}\right) = 2.42\ d/\ell. \tag{E29}$$

If the standard KM relations (E26) were used with these numerical values, the relations (E25) would read

$$R_\infty = 0.61,\quad \ell n\left(\frac{1-R_dR_\infty}{1-R_d/R_\infty}\right) = 0.825\ d/\ell \tag{E30}$$

which are significantly in error. On the other hand, if the incorrect solutions (E23) were used in the boundary value problem, without requiring $|q_{1,2}|<<1$, R_∞ would come out to be the correct value (E29), since it does not depend on $p_{1,2}$. However, the second relation in (E25) would be

$$\ell n\left(\frac{1-R_dR_\infty}{1-R_d/R_\infty}\right) = (q_1-q_2)\ \frac{d}{\ell} = 3.1\ d/\ell,$$

different from both the second relations in (E29) and in (E30).

In sum, in this appendix it has been shown that, for a one-dimensional random scattering medium,

i) Radiative transfer equations follow directly from wave theory equations if there is zero phase correlation among the waves incident on any scatterer from different directions.

ii) The correct radiative transfer equations are difference rather than differential equations.

This latter point is exploited in Appendix I.

APPENDIX F

CONVERSION OF FRACTION BY WEIGHT TO NUMBER DENSITY

In a multi-constituent random scattering medium, the given data are invariably the total mass density, D, of the actual medium, and the fraction by weight, p_i, of each constituent number $\underline{i}$. For use in Mie theory algorithms, it is necessary to know the number density N_i of each of the constituent particles.

Let ρ_i be the mass density of particles of type i, and v_i be the average volume of a type i particle. Then, for a sample with total mass M, total volume V, mass m_i of i^{th} constituent, and $n_i \equiv$ total number of type $\underline{i}$ particles,

$$\frac{m_i}{V} = \frac{m_i}{M}\,\frac{M}{V} = p_i D = \frac{n_i \rho_i v_i}{V} = N_i \rho_i v_i. \tag{F1}$$

Solving this for N_i yields

$$N_i = p_i D/\rho_i v_i. \tag{F2}$$

Now

$$v_i = \int dr\, f_i(r)(4\pi r^3/3), \tag{F3}$$

where $f_i(r)$ is the size distribution of type i particles. Therefore, in order to evaluate N_i, the size distributions must also be given.

APPENDIX G

SIZE DISTRIBUTIONS

Four well-known particle size distributions[4] were programmed for use in this work. These are the two-parameter gamma distribution, the bimodal gamma distribution, the log-normal distribution, and a power law distribution. The unnormalized distributions, n(r), and the normalized ones, f(r), are defined and described below.

i) Two-parameter gamma distribution

$$n(r) = \begin{cases} r^{1/b}\, r^{-3} \exp-(r/ab), & r_1 \le r \le r_2 \\ 0 \qquad\qquad\qquad\qquad , & r < r_1;\ r > r_2 \end{cases} \qquad \text{(G1)}$$

If $r_1 = 0$, $r_2 = \infty$, then

$$a = 3\langle r\rangle - 2r_o,\quad b = \sigma^2/(1+2\sigma^2),\quad \sigma^2 \equiv (\langle r^2\rangle - \langle r\rangle^2)/\langle r\rangle^2$$

where r_o = modal radius = a - 3ab, $\langle r\rangle$ = mean radius = a-2ab, $\langle r^2\rangle$ = mean square radius = $(ab)^2(\frac{1}{b} - 1)(\frac{1}{b} - 2)$. If $r_1 > 0$, or $r_2 < \infty$, or both, then the relations between ($\langle r\rangle$, $\langle r^2\rangle$) and (a,b) are altered, but r_o = a-3ab unless $r_1 > r_o$ or $r_2 < r_o$.

ii) Bimodal gamma distribution

$$n(r) = \frac{n(r,a_1,b)}{\int_{r_1}^{r_2} dr\ n(r,a_1,b)} + \frac{n(r,a_2,b)}{\int_{r_1}^{r_2} dr\ n(r,a_2,b)}, \qquad \text{(G2)}$$

where $n(r,a_i,b)$ is a two-parameter gamma distribution with parameters (a_i,b). Here, half of the particles are in each mode.

iii) Log normal distribution

$$n(r) = \left\{ \begin{array}{ll} r^{-1} \exp[1-(\ell n\ r/r_g)^2/2\sigma^2], & r_1 \le r \le r_2 \\ 0 & , \ r<r_1,\ r>r_2 \end{array} \right\} \quad . \tag{G3}$$

If $r_1 = 0$, $r_2 = \infty$, then

$$\langle r \rangle = r_g e^{-\sigma^2/2},\ \langle r^2 \rangle = r_g^2\, e^{-2\sigma^2},\ r_o = r_g\, e^{-\sigma^2} = \langle r^2 \rangle^{1/2},$$

and $\left|(\langle r^2 \rangle - \langle r \rangle^2)/\langle r \rangle^2\right| = 1-e^{-\sigma^2}$. If $r_1 > 0$, or $r_2 < \infty$, or both, these relations are altered.

iv) Power law distribution

$$n(r) = \left\{ \begin{array}{ll} r^{-a}, & r_{min} \le r \le r_{max} \\ 0 & , \ r < r_{min},\ r > r_{max} \end{array} \right\} \tag{G4}$$

here $$\langle r \rangle = \frac{1-a}{2-a}\ \frac{r_{max}^{2-a} - r_{min}^{2-a}}{r_{max}^{1-a} - r_{min}^{1-a}},\ a \neq 1,2.$$

$$\langle r \rangle = \frac{r_{max}^{2-a} - r_{min}^{2-a}}{(2-a)\,\ell n(r_{max}/r_{min})},\ a = 1$$

$$\langle r \rangle = \frac{(1-a)\,\ell n(r_{max}/r_{min})}{r_{max}^{1-a} - r_{min}^{1-a}},\ a = 2.$$

The normalized distributions f(r) were calculated numerically from

$$f(r) \equiv n(r) \Big/ \int_{r_1}^{r_2} dr\ n(r). \tag{G5}$$

Several other distributions could be added easily to the computer program.

APPENDIX H

$p^{(o)}(\mu,\mu')$ FROM $p(\cos\Theta)$

In this work, the single scattering phase function $p(\cos\Theta)$ was first calculated from Mie theory for some set of scattering angles Θ_k, $k = 1,\ldots, L$. What is needed for multiple scattering calculations in this study is the azimuth-averaged phase function

$$p^{(o)}(\mu,\mu') = \frac{1}{2\pi}\int_o^{2\pi} d\phi'\ p(\cos\Theta), \tag{H1}$$

on some set (μ_i,μ_j), $i,j = 1,\ldots, N$. Here,

$$\cos\Theta = \mu\mu' + \sqrt{1-\mu^2}\ \sqrt{1-\mu'^2}\ \cos\phi'. \tag{H2}$$

The method used in this work to obtain $p^{(o)}(\mu,\mu')$ is that of Hansen[15] and Hansen and Travis[4]. First, choose the particular (μ_i,μ_j') values desired. For each pair of values, do the integration in Eq. (H1) numerically. For example, using Gauss-Legendre quadrature on the points $\phi' = \phi_n$, with weights w_n, $n=1,\ldots,Q$,

$$\bar{p}^{(o)}(\mu_i,\mu_j') = \sum_{n=1}^{Q} w_n p(\mu_i\mu_j' + \sqrt{1-\mu_i^2}\ \sqrt{1-\mu_j'^2}\ \cos\phi_n). \tag{H3}$$

However, the value $\cos\Theta_{nij} = \mu_i\mu_j' + \sqrt{1-\mu_i^2}\ \sqrt{1-\mu_j'^2}\ \cos\phi_n$ might not be one of the $\cos\Theta_k$ for which $p(\cos\Theta_k)$ was calculated. If not, linear interpolation is used between the two adjacent $\cos\Theta_k$ to find $p(\cos\Theta_{nij})$. After $\bar{p}^{(o)}(\mu_i,\mu_j')$ is found by this method on all points (μ_i,μ_j') which are desired, it is renormalized by using

$$p^{(o)}(\mu,\mu') \equiv \omega_o \bar{p}^{(o)}(\mu,\mu') / \int_{-1}^{1} d\mu \, \bar{p}^{(o)}(\mu,\mu'). \qquad (H4)$$

The function $p^{(o)}(\mu,\mu')$ so defined is thus correctly normalized to ω_o. This renormalization helps to remove errors that may have been introduced by the interpolation.

This method of obtaining $p^{(o)}(\mu,\mu')$ is considerably faster computationally than the method which uses Legendre function expansions, for a given accuracy.

APPENDIX I

NEW EQUATION OF RADIATIVE TRANSFER

In the usual derivation[5] of the standard RT equation (A9), there is no analog to the difference equations (E16). However, the derivation of Eq. (A9) given in Appendix A does pass through such an analog, namely, Eq. (A6). The considerations in Appendix E lead to the conclusion that the difference equation (A6) ought to be a more accurate radiative transfer equation than the standard differential equation (A9), for close-packed strongly absorbing or strongly reflecting media. Therefore, (A6) is tentatively considered as the new equation of radiative transfer.

In what follows, consider only problems which are invariant to translations normal to the z-direction. Then, the intensities in Eq. (A6) may be written $I(z+\ell\mu/2,\mu,\phi)$, etc., where μ is the cosine of the angle between $\underset{\sim}{s}$ and the z-direction, and ϕ is the azimuthal angle of $\underset{\sim}{s}$ around the z-axis. For applications in which only the total transmitted and reflected fluxes are needed, the ϕ-dependence of Eqs. A6 may be integrated out, just as was done in going from Eq. (A16) to Eq. (A18). Eq. (A6) then reduces to

$$I(z+\ell\mu/2,\mu) = (1-\gamma\ell)I(z-\ell\mu/2,\mu)+(\gamma\ell/2)\int_{-1}^{1} d\mu'\ p^{(o)}(\mu,\mu')I(z-\ell\mu'/2,\mu'). \tag{I1}$$

Since z is a continuous variable, let $z \to z + \ell\mu/2$ in Eq. (I1). The resulting equation is

$$I(z+\ell\mu,\mu) = (1-\gamma\ell)I(z,\mu) + (\gamma\ell/2)\int_{-1}^{1} d\mu'\ p^{(o)}(\mu,\mu')I((z+\tfrac{1}{2}\ell(\mu-\mu'),\mu'). \tag{I2}$$

Let there be an incident beam in direction μ_o at $z = 0$, so that

$$I_{in}(o,\mu) = \frac{1}{2}\ F\ \delta(\mu-\mu_o). \tag{I3}$$

Then, let $I_{in}(z,\mu)$ satisfy $I(z+\ell\mu,\mu) = (1-\gamma\ell)\ I(z,\mu)$. Then

$$I_{in}(z,\mu) = \frac{1}{2}\ F\ \delta(\mu-\mu_o)\ \exp[z\ \Gamma(\mu)], \tag{I4}$$

where

$$\Gamma(\mu) = (\mu\ell)^{-1}\ \ell n(1-\gamma\ell); \tag{I5}$$

note that, for $\gamma\ell<<1$, $\Gamma(\mu) \simeq -\gamma/\mu$, the usual form. Then, let

$$I(z,\mu) = I_{in}(z,\mu) + I_{di}(z,\mu) \tag{I6}$$

in Eq. (I2), where $I_{di}(z,\mu)$ is the diffuse intensity. This yields

$$I_{di}(z+\ell\mu,\mu) = (1-\gamma\ell)I_{di}(z,\mu) + (\gamma\ell\ F/4)p^{(o)}(\mu,\mu_o)\ \exp[\Gamma(\mu_o)(z+\tfrac{1}{2}\ell(\mu-\mu_o))]$$
$$+ (\gamma\ell/2)\int_{-1}^{1} d\mu'\ p^{(o)}(\mu,\mu')I_{di}(z+\tfrac{1}{2}\ell(\mu-\mu'),\mu'). \tag{I7}$$

This difference equation is the analog of the differential equation (A19).

It is not clear how to solve this equation by a doubling method, which depends on the choice of a starting layer so thin that the last term above may be dropped for the transfer across that layer (see Appendix J). Here, the minimum thickness layer which can be chosen in

principle is one of thickness ℓ, because that is the thickness of a monoparticle layer, and the whole derivation of the equations in terms of particle cross-sections probably makes no sense for thinner layers. Now, if $\gamma\ell \ll 1$, which implies that both $\alpha \ll 1$, $\beta \ll 1$, then the difference equation (I7) reduces to the standard differential equation (A21). But, if accuracy of 1% or better is desired, then the conventional equation (A21) should not be used for $\gamma\ell \geq 0.01$.

A many-flux solution, similar to that done by Mudgett and Richards[10] for the standard differential equation, may certainly be done; this is quite cumbersome and time-consuming for more than four fluxes. However, a combination of an accurate many-flux (16 or 32-flux might be sufficient) solution for the starting layer of thickness ℓ, with a doubling method solution for the larger thicknesses desired, seems feasible.

A Monte Carlo solution is of course possible. In fact, it seems likely that the standard Monte Carlo technique is already solving this difference equation, rather than the usual differential equation, inasmuch as the Monte Carlo technique looks at the radiative transfer collision by collision. If so, discrepancies should exist between Monte Carlo method results and results of other methods for the standard equation, for closely packed media containing strongly absorbing or strongly reflecting particles. This point remains to be checked in future work.

The two-flux theory of Equation (I2) may be obtained in a manner similar to that in which two-flux theory of Eq. (A18), the KM

theory, was obtained in Appendix B. Make the approximations

$$I(z+\ell\mu,\mu) \simeq I_+(z+\ell\bar{\mu}) = I_+(z+\ell/2),\ \mu > 0$$
$$I(z-\ell\mu,-\mu) \simeq I_-(z-\ell\bar{\mu}) = I_-(z-\ell/2),\ \mu > 0 \tag{I8}$$

where the second equalities follow from the definition $\bar{\mu} \equiv \int_0^1 d\mu\ \mu = \frac{1}{2}$. Then Eq. (I2) reduces to the pair of coupled equations

$$I_+(z+\ell/2) = [1-(\alpha+\beta_-)\ell]I_+(z)+(\beta_-\ell)I_-(z+\ell/2),$$
$$I_-(z) = (\beta_-\ell)I_+(z) + [1-(\alpha+\beta_-)\ell]I_-(z+\ell/2), \tag{I9}$$

where

$$\beta_\pm \equiv \frac{\gamma}{2}\int_0^1 d\mu \int_0^1 d\mu'\ p^{(o)}(\mu,\pm\mu'), \tag{I10}$$

just as in Appendix B, and α, β, γ have the same meanings as in Appendix A, with $\beta_+ + \beta_- = \beta$, so $\gamma-\beta_+ = \alpha+\beta_-$.

Define, as in Appendix B,

$$\Phi_\pm(z) \equiv \int_0^1 d\mu\ \mu\ I_\pm(z) = \frac{1}{2}\ I_\pm(z). \tag{I11}$$

Then Eqs. (I9) reduce to

$$\Phi_+(z+\ell/2) = T\ \Phi_+(z) + R\ \Phi_-(z+\ell/2)$$
$$\Phi_-(z) = R\ \Phi_+(z) + T\ \Phi_-(z+\ell/2) \tag{I12}$$

where

$$T \equiv 1-(\alpha+\beta_-)\ell,\ R \equiv \beta_-\ell,\ \Lambda \equiv \alpha\ell, \tag{I13}$$

satisfy A + R + T = 1, and have the significance (T, R, A) = (transmission, reflection, absorption) fractions for a layer of thickness $\ell/2$. The presence of $\ell/2$ rather than ℓ in the arguments of $\Phi_{\pm}$ is a result of the averaging over μ done in obtaining Eqs. (I9). Note that, if $R \ll 1$, $A \ll 1$, then Eqs. (I12) reduce to the KM equations (B1), as expected; the presence of $\ell/2$ rather than ℓ in (I12) is crucial for this.

Solving these equations for $\Phi_{\pm}(z+\ell/2)$ in terms of $\Phi_{\pm}(z)$ yields

$$\begin{aligned} \Phi_+(z+\ell/2) &= (1-a)\Phi_+(z)+b\ \Phi_-(z) \\ \Phi_-(z+\ell/2) &= -b\ \Phi_+(z) + (1+c)\Phi_-(z) \end{aligned} \tag{I14}$$

where

$$a \equiv (T-T^2+R^2)/T,\ b \equiv R/T,\ c \equiv (1-T)/T, \tag{I15}$$

just as in Eqs. (E17). Since these difference equations (I14) have the same form as the Eqs. (E16), the results and solutions of Eqs. (E16) may be applied directly here. The solutions are

$$\begin{aligned} \Phi_+(z) &= A_{+1}\, e^{p_1 z} + A_{+2}\, e^{p_2 z}, \\ \Phi_-(z) &= b^{-1}[(a+q_1)\, A_{+1}\, e^{p_1 z} + (a+q_2) A_{+2}\, e^{p_2 z}], \end{aligned} \tag{I16}$$

where A_{+1}, A_{+2} are undetermined coefficients, and where

$$\begin{aligned} p_{1,2} &= \frac{2}{\ell}\, \ell n\ (1 + q_{1,2}), \\ q_{1,2} &= \frac{1}{2}\ (c-a) \pm [(c-a) + \frac{1}{4}\ (c-a)^2]^{1/2}. \end{aligned} \tag{I17}$$

For a slab of thickness d on a totally absorbing background,

$$R_\infty = (a+q_2)/b \; ; \quad (p_1-p_2)d = \ell n \left(\frac{1-R_d R_\infty}{1-R_d/R_\infty}\right). \tag{I18}$$

These are just the results E19-E21 and E25, except for the factor of 2 in the definitions of $p_{1,2}$. If $T \lesssim 1$, $R \ll 1$, $A \ll 1$, Eqs. (I18) go over to the KM Theory expressions (B2).

A few examples are most instructive here, and show that, in some practical problems, the results predicted by the corrected equations (I14, I18) differ significantly from those predicted by the standard KM equations (B1, B2).

i) Consider a powder made up of small carbon particles. For such particles, $R \ll 1$, but $A \lesssim 1$, so $T \ll 1$. Let $T = 1-A-R$, so, from Eq. (I15),

$$c-a = \frac{(A+R)^2 + R^2}{1-A-R} \simeq \frac{A^2}{1-A} + \frac{RA(2-A)}{(1-A)^2} \tag{I19}$$

to $0(R)$. Then, for $A \simeq 1/2$, say, c-a is not $\ll 1$, so $q_{1,2}$ is quite different from $(c-a)^{1/2}$, and $p_{1,2} \neq 2q_{1,2}/\ell$. This means that the relations (I18), among (R_∞, R_d) and the coefficients (β_-,α), are quite different from the KM relations (B2). A value of $A \gtrsim 1/2$ is quite realistic for carbon powder.

ii) Consider the model powders treated in this work. In all of these, the strongly reflecting $BaSO_4$ was by far the majority component. For example, in sample II, $BaSO_4$ + carbon, the values of (β_-,α,ℓ) may be found from Tables 2, 3, at wavelength $\lambda = 0.6$ μm:

$$\alpha = 5.21\times10^{-4}\ (\mu m)^{-1},\ \beta_- = 0.102(\mu m)^{-1},\ \ell = N^{-1/3} = 2.77\ \mu m.$$

Therefore, from Eqs. (I13),

$$R \simeq 0.283,\ A = .513\times10^{-4},\ T = 1-R-A.$$

Since $A << 1$, we expand the parameters (a,b,c) of Eqs. (I15) to O(A). The results are

$$c-a = \frac{2RA}{1-R}\ ,\ a = \frac{R}{1-R} + \frac{A(1-2R+2R^2)}{(1-R)^2}\ ,$$

$$b = \frac{R}{1-R} + \frac{RA}{(1-R)^2}\ ,\ q_{1,2} \simeq \pm\ (\frac{2RA}{1-R})^{1/2} << 1,\ p_{1,2} \simeq 2q_{1,2}/\ell.$$

Then, from Eqs. (I12)

$$R_\infty = 1-(\frac{2A(1-R)}{R})^{1/2},\ \frac{4d}{\ell}(\frac{2RA}{1-R})^{1/2} = \ell n(\frac{1-R_dR_\infty}{1-R_d/R_\infty}).$$

Solving these for A/R and R yields

$$(\frac{1-R}{R})A = \frac{(1-R_\infty)^2}{2}\ ;\ \frac{4d}{\ell}\ (\frac{R}{1-R}) = \frac{1}{1-R_\infty}\ \ell n(\frac{1-R_dR_\infty}{1-R_d/R_\infty}). \qquad (I20)$$

These relations are to be contrasted with Eqs. (B2) of the KM theory, which, for $A<<1$, yield

$$\frac{A}{R} = \frac{K}{S} = \frac{(1-R_\infty)^2}{2}\ ;\ \frac{4d}{\ell}\ R = \frac{1}{1-R_\infty}\ \ell n(\frac{1-R_dR_\infty}{1-R_d/R_\infty}). \qquad (I21)$$

Note that $A = \alpha\ell = K\ell/2$, $R = \beta_-\ell = S\ell/2$. Comparison of (I20, I21) makes it clear that, for given data (R_d,R_∞),

$$(\frac{R}{1-R})_{new} = (R)_{KM}\ ;\ \text{or}\ R_{new} < R_{KM},\ \text{but}$$

$$(A)_{new} = (A)_{KM}.$$

That is, the KM theory prediction of R is too high, by a factor $1/(1-0.283) \simeq 1.4$ in this numerical example, but the KM theory prediction of A agrees with that of the corrected theory. This latter equality is fortunate for the main purpose of this work, which was to check the supposed equality of the KM coefficient $\bar{K} = 2A/\ell$, calculated from the KM eqs. (B2), with the absorption coefficient 2α. Note well that even though $|q_{1,2}| \ll 1$ in this example, the results do not agree with those of the KM theory; for this agreement it must be true that both $A \ll 1$, $R \ll 1$, which was not the case in either of these examples.

It is worth remarking that, for very strongly reflecting particles, especially for such particles of large radius, the usual assumption of neglecting the multiple scattering in a monoparticle layer may be invalid. This assumption was implicit in the above derivation of the corrected two-flux equations. In order to take into account such effects, at least a 3-flux set of equations must be used, or, for accuracy, a many-flux set. It is also likely that the conventional reasoning which allows replacement of all the different particles in the medium by average particles (see Appendix A) needs to be reexamined if $\gamma\ell \to 1$. These are topics for future work.

In sum, the above two-flux theory of the difference equations (I2), and the two-flux theory of the differential equation (A18), (the KM theory), yield significantly different results, for strongly absorbing or strongly reflecting closely packed media. This implies that the accurate solutions of Eq. (I7) and Eq. (A19) will be significantly different, for such media.

Previous attempts by other authors at discontinuous theories of radiative transfer are outlined in reference (13). These theories are only the two-flux approximations, and the individual particle scattering and absorption cross-sections do not seem to be an integral part of the development, although the philosophy of these theories is similar to that of the new theory presented here.

APPENDIX J

DOUBLING METHOD

In this appendix, the doubling method equations used in this work are derived. The fundamental transmission equations for a plane parallel layer of thickness ℓ (optical thickness $\tau = \gamma\ell$) may be written

$$I_+(d,\mu) = \int_0^1 d\mu' [T_\ell(\mu,\mu') I_+(o,\mu') + R_\ell(\mu,\mu') I_-(d,\mu')]$$

$$I_-(o,\mu) = \int_0^1 d\mu' [T_\ell(\mu,\mu') I_-(d,\mu') + R_\ell(\mu,\mu') I_+(o,\mu')] \tag{J1}$$

where $\mu \geq 0$, and

$$I_\pm(z,\mu) \equiv \sqrt{\mu}\, I_\pm(z,\mu). \tag{J2}$$

Here, $I_\pm(z,\mu)$ are the total intensities, diffuse plus directly transmitted, averaged over azimuthal angle ϕ, and are defined by

$$I_+(z,\mu) = I(z,\mu),\ \mu>0;\ I_-(z,\mu) \equiv I(z,-\mu),\ \mu>0. \tag{J3}$$

In symbolic operator form, Eqs. (J1) may be written

$$I_+(\ell) = T_\ell\ I_+(o) + R_\ell\ I_-(\ell)$$

$$I_-(o) = T_\ell\ I_-(\ell) + R_\ell\ I_+(o). \tag{J4}$$

Consider another layer of thickness d, between $z = \ell$ and $z = 2\ell$. Then

$$I_+(2\ell) = T_\ell\ I_+(\ell) + R_\ell\ I_-(2\ell)$$

$$I_-(\ell) = T_\ell\ I_-(2\ell) + R_\ell\ I_+(\ell). \tag{J5}$$

But, for the total thickness 2ℓ,

$$I_+(2\ell) = T_{2\ell}\, I_+(o) + R_{2\ell}\, I_-(2\ell)$$
$$I_-(o) = T_{2\ell}\, I_-(2\ell) + R_{2\ell}\, I_+(o). \tag{J6}$$

Combining these sets of equations yields

$$T_{2\ell} = T_\ell(1-R_\ell R_\ell)^{-1}T_\ell;\ R_{2\ell} = R_\ell + T_\ell(1-R_\ell R_\ell)^{-1}R_\ell T_\ell,$$

which are the doubling equations in operator form. For example,

$$T_\ell T_\ell \equiv \int_o^1 d\mu'\ T_\ell(\mu,\mu')\int_o^1 d\mu''\ T_\ell(\mu',\mu'')(\ldots), \tag{J7}$$

where the ellipsis (...) stands for the operand, some function of μ''. The operator $(1-R_\ell R_\ell)^{-1}$ is defined by its series expansion,

$$(1-R_\ell R_\ell)^{-1} \equiv 1+R_\ell R_\ell + R_\ell R_\ell R_\ell R_\ell + \ldots$$
$$= \int d\mu'\ \delta(\mu-\mu')(\ldots) + \int d\mu'\ R_\ell(\mu,\mu')\int d\mu''\ R_\ell(\mu',\mu'')(\ldots) + \ldots \tag{J8}$$

In practical computation, ten or fewer terms are kept in the above series, and an estimate of round-off error is included, following the method of Hansen and Travis[4].

In order to make use of the doubling equations, the transfer matrices T_ℓ, R_ℓ for a very thin layer of thickness ℓ, so thin that multiple scattering may be neglected, must be found. For such a layer, the scattering term, $\frac{1}{2}\gamma\int d\mu'\ p^{(o)}(\mu,\mu')I_{di}(z,\mu')$, is dropped from Eqs. (A19), and the resulting equation is solved analytically. The T_ℓ, R_ℓ may be read off from these solutions; they turn out to be

$$T_\ell(\mu,\mu') = \frac{p(\mu,\mu')}{2(\mu\mu')^{1/2}}\left(\frac{1}{\mu}-\frac{1}{\mu'}\right)^{-1}\left(e^{-\gamma\ell/\mu'}-e^{-\gamma\ell/\mu}\right) + \delta(\mu-\mu')e^{-\gamma\ell/\mu}$$

$$R_\ell(\mu,\mu') = \frac{p(\mu,-\mu')}{2(\mu\mu')^{1/2}}\left(\frac{1}{\mu}+\frac{1}{\mu'}\right)^{-1}\left[1-\exp-\gamma\ell\left(\frac{1}{\mu}+\frac{1}{\mu'}\right)\right]. \tag{J9}$$

These expressions are finite for all μ,μ', but considerable care must be taken in computation as either μ or $\mu' \to 0$, or as $\mu \to \mu'$.

Numerical integration over δ-function integrands can lead to significant error. It was judged more accurate to write

$$T_\ell = T_{\ell,di} + T_{\ell,in} \tag{J10}$$

at each step of the doubling, where $T_{\ell,in}$ contains the δ-function operator. This expands the equation for $T_{2\ell}$ to four terms, and that for $R_{2\ell}$ to five. For doubling from a thickness L to a thickness 2L, there results

$$T_{2L} = T_{2L,di} + \delta(\mu-\mu')e^{-2\gamma L/\mu};\ T_L = T_{L,di} + \delta(\mu-\mu')e^{-\gamma L/\mu}, \tag{J11}$$

where $T_{2L,di}$, $T_{L,di}$ contain all the terms not proportional to $\delta(\mu-\mu')$.

If the incident intensity is $\delta(\mu-\mu_o)$, then the incident flux is μ_o. For a sample of thickness d, the diffuse transmitted and reflected fluxes are

$$\Phi_{+di} = \int d\mu\sqrt{\mu}\ I_+(D,\mu) = \int_o^1 d\mu\sqrt{\mu}\ T_{d,di}(\mu,\mu_o)\sqrt{\mu_o}$$

$$\Phi_{-di} = \int d\mu\sqrt{\mu}\ I_-(D,\mu) = \int_o^1 d\mu\sqrt{\mu}\ R_{d,di}(\mu,\mu_o)\sqrt{\mu_o} \tag{J12}$$

and the directly transmitted flux is $\mu_o e^{-\gamma d/\mu_o}$. Therefore, the transmittances and reflectance are

$$T_{direct} = e^{-\gamma d/\mu_o},\ T_{di} = \int_o^1 d\mu(\mu/\mu_o)^{1/2}\, T_{d,di}(\mu,\mu_o),\ R = \int_o^1 d\mu(\mu/\mu_o)^{1/2} R_{d,di}(\mu,\mu_o).$$

For a pure scattering medium (no absorption), it must be true that

$$T_{direct} + T_{di} + R = 1. \qquad \text{(J14)}$$

This relation was used as an internal check on the computational accuracy.

APPENDIX K

COMPUTER PROGRAMS

Two computer programs were developed during the course of this investigation, one based on the Mie theory, the other on conventional multiple scattering theory. A short description of each program is given in this appendix. Complete documentation and listings are available from the author.

Both programs use Gauss-Legendre quadrature and double precision arithmetic throughout, and both were thoroughly checked for accuracy. The Mie scattering program was checked against published results,[4] and against analytic results, and it was verified that, as the model sample particles are taken further and further apart, the near field phase function (Appendix A) approaches the far field one. The multiple scattering program agrees with the results of an analytic calculation[16], and satisfies internal checks for all optical depths ≤ 1024.

1. Mie Scattering Program

Given the mass density of a model mixture of spherical particles, and the optical constants, size distribution, and fraction by weight of each component in the mixture, this program calculates the number density of the mixture; the number density, near and far field differential cross-section, and the extinction, scattering, and absorption cross-sections for each component of the mixture, and for the mixture as a whole, using standard Mie theory algorithms, and the procedures explained in Appendices A and F. It also calculates the phase functions on a chosen set of scattering angles Θ.

A detailed description of a typical Mie theory scattering calculation is readily available in the current literature[3,4]. The major differences between the program developed for this work and the PGAUSS routine[17] are as follows:

i) The logarithmic derivatives of $\psi_n(z)$, rather than the $\psi_n(z)$ functions themselves, were computed by backward recursion.[18,19] Here, the $\psi_n(z)$ are the Riccati-Bessel functions, the notation that of Van de Hulst[3].

ii) The output of the program yields the phase function $p(\Theta)$ on a selected set of scattering angles Θ, not the coefficients of the Legendre polynomials in the standard series expansion of the phase function.

2. Multiple Scattering Program

This program uses the punched output (mixture phase function, $p(\Theta)$) from the Mie scattering program, and computes the diffuse reflectance and transmittance as functions of the angle θ_o of the incident beam and the plane-parallel sample optical thickness, using the doubling method (Appendix J) to solve the standard radiative transfer equation (A21). The program then uses these calculated reflected fluxes in the KM formulas (B2) in order to compare directly the predicted values $(\bar{K},\bar{S})$ with the defined values $K \equiv 2\alpha$, $S \equiv 2\beta_-$. The program also calculates the quantities $\beta_\pm$, $P_\pm(\mu_o)$, defined in Appendices B and C. The phase function $p^{(o)}(\mu,\mu')$ is obtained from the input $p(\Theta)$ by the method described in Appendix H.